Hyperglycemia Increases Mitochondrial Protein Expression in the Absence of Oxidative Stress

By

Francisco E. Vasquez

Submitted to the department of Pharmacology & Toxicology and the Faculty of the Graduate School of the University of Kansas in partial fulfillment of the requirements for the degree of Master of Science.

Thesis Committee:

_____

Rick T. Dobrowsky, Ph.D, Professor and Chair of the Thesis Committee

_____

Jackob Moskovitz, Ph.D, Assistant Professor and Thesis Committee Member

_____

Jeff Staudinger, Ph.D,Associate Professor and Thesis Committee Member

Thesis defended: 9th December, 2008

The Thesis Committee for Francisco E. Vasquez certifies
that this is the approved Version of the following thesis:

Hyperglycemia Increases Mitochondrial Protein Expression in the Absence of Oxidative Stress

Thesis Committee:

_____
Rick T. Dobrowsky, Ph.D, Professor and Chair of the Thesis Committee

_____
Jackob Moskovitz, Ph.D, Assistant Professor and Thesis Committee Member

_____
Jeff Staudinger, Ph.D, Associate Professor and Thesis Committee Member

Thesis defended: 9th December, 2008

Abstract

Long-term diabetes may cause diabetic peripheral neuropathy (DPN). Hyperglycemic-induced oxidative stress is widely accepted as the contributing factor in the development of diabetic complications. The mitochondrion has been singled out as the site of increased production of superoxide (O_2^-). Oxidative stress has been shown to be particularly deleterious to mitochondria because it is intimately associated with apoptosis. We utilized proteomics to study the effect chronic hyperglycemia may have on enriched Schwann Cell (SC) mitochondria. Through stable isotope labeling of amino acids in cell culture (SILAC) and mass spectrometry we were able to determine that chronic hyperglycemia induced an overexpression of proteins important in detoxification that occurred independently from oxidative stress. We conclude that the SCs under hyperglycemic stress react by increasing the levels of protective proteins to counter the influx of high glucose thus affording *protection* not only for itself but the crucial axon it enwraps.

Acknowledgments

The common person,

Through your tax dollars such work before you is possible.

I doubt you will ever read this piece of scientific work, since you rarely have the time and interest to understand matters that concern you.

You always allow a few to seek answers to life's great mysteries.

The common person, get involved!

I am grateful to the University of Kansas for supplying exceptional equipment to conduct all my experiments.

I am grateful to Rick T. Dobrowsky for competing for the funding that made this research possible.

This work is also an act showing deep respect for my father.

Table of Contents

List of Figures

List of Abbreviations

AGEs – Advanced Glycation End Products
APs – Action Potentials
AR – Aldose Reductase
ARI – Aldose Reductase Inhibitor
ATP- Adenosine-5'-Triphosphate
CAD- Coronary Artery Disease
DCCT – Diabetes Control and Complication Trial
dFCS – Dialyzed Fetal Calf Serum
DHE- Dyhroethidium
DMEM- Dubelco's Modified Eagles Medium
DMSO- Dimethyl Sulfoxide
DPN – Diabetic Peripheral Neuropathy
DTT- Dithiothreitol
DRGs- Dorso Root Ganglion
EDIC – Epidemiology of Diabetes Intervention and Complications Study
EDTA - Ethylenediaminetetraacetic Acid
ER- Endoplasmic Reticulum
$FADH_2$ - Flavin Adenine Dinucleotide
FBS- Fetal Bovine Serum
GRP78- Glucose-Regulated Protein
GSH – Reduced Glutathione
GSSH – Oxidized Glutathione
H_2O_2 – Hydrogen Peroxide
HEPES - 4-(2-hydroxyethyl)-1-Piperazineethanesulfonic Acid
HEK- Human Embryonic Kidney Cells
HM- Heavy Mitochondria Fraction
LDH- Lactate Dehydrogenase
Leu-d3 – Deuterated Leucine
LTQ-FT MS/MS - Hybrid Linear Quadrupole Ion Trap Fourier Transform Ion Cyclotron Resonance Tandem Mass Spectrometer
MIBA – Mitochondrial Isolation Buffer
MnSOD – Manganse superoxide dismutase
MPT – Mitochondrial Permeability Transition
NADH – Nicotinamide Adenine Dinucleotide
NADPH – Nicotinamide Adenine Dinucleotide Phosphate – Oxidase
NF-kB – Nuclear Factor-kB
NO – Nitric Oxide
O_2^- - Superoxide
$ONOO^-$ - Peroxynitrite
p62 - Nucleoporin

PAD – Peripheral Arterial Disease
PBS - Phosphate-Buffered Saline
PBST- Phosphate-Buffered Saline with Tween
PNS- Peripheral Nervous System
PT- Permeability Transition
RAGE – Receptor for Advanced Glycation End Products
ROS- Reactive Oxygen Species
RP-HPLC – Reverse-Phase High Performance Liquid Chromatography
SCs – Schwann Cells
SDH – Sorbitol Dehydrogenase
SDS-PAGE- Sodium Dodecyl Sulfate Polyacrylamide Gel Electrophoresis
SILAC – Stable Isotope Labeling with Amino Acids in Cell Culture
sRAGE –Recombinant Soluble Form of RAGE
STZ- Streptozotocin
TCA cycle – Tricarboxylic Acid Cycle
TPP – Techno Plastic Products
VEGF – Vascular Endothelial Growth Factor
WST-1 – Water Soluble Tetrazolium Salt
XO- Xanthine Oxidase

Introduction

Diabetes is a prevalent metabolic disorder in both developed and developing countries. In the U.S alone, 8% of the population has diabetes, a statistic primarily represented by two major age groups affected by the disease; 20 years and older and 60 years and older [1]. Genetics and increasing rates of obesity are major factors influencing the rates of type I and II diabetes [2]. Type I diabetes is the most severe form of the disease because the administration of insulin therapy is a requirement for the patient's body to convert glucose into energy. Type II diabetes although the most common is treated by altering lifestyle and dietary habits at the onset of the disease and at disease progression more intrusive methods of administering medications such as Metformin, sulfonylureas, and insulin therapy may be necessary [3]. Due to a good understanding of diabetes, i.e., advising patients to maintain blood glucose concentration levels less than 5.6 mmol/L, type I and II patients are able to live long and prosperous lives [4]. An important caveat of prolonging the life of both types of diabetic patients is the inevitable fate of developing secondary complications. The diabetes control and complications trial (DCCT) a prospective, multi-centre, randomized trial conducted in medical and educational institutions in the U.S. and Canada definitely proved that tight glycemic control is the best method to prevent the onset of secondary complications of diabetes. The investigators found that intensive therapy, 3 or more insulin injections followed by frequent glucose monitoring, reduces the risk of developing retinopathy by 76% and clinical neuropathy by 60%

[5]. Moreover, the Epidemiology of Diabetes Intervention and Complications study (EDIC), an extension to the 6.5 year DCCT, showed that subjects who remained under intensive therapy for an additional 8 years had significantly less symptoms and signs of clinical neuropathy compared to the conventional group of subjects who 14.5 years earlier were instructed to administer one or two insulin injections per day [6].

The importance of preventing diabetic peripheral neuropathy (DPN) cannot be overstated. The poor management of diabetes due to busy work schedules, lack of motivation, bad education, or issues of non-compliance prolonged glucose dysregulation will eventually lead to DPN. The most common form of DPN is chronic distal symmetrical polyneuropathy that affect the cell body of neurons, axon and myelin resulting in slowed nerve conduction velocities [7]. The slowing of axonal action potential conduction has been attributed to demyelination of the Schwann cells (SCs) and is commonly associated with positive sensory symptoms such as numbness and pain [8]. The onset of DPN leads to serious medical complications such as loss of sensation to the lower extremeties and muscle weakness that is commonly accompanied by microvascular insults that reduce blood flow to the peripheral limbs leading to ulceration due to a laceration [9]. Neuropathies and microvascular insults result in a combination of pathologies that may lead to the amputation of a lower extremity and a significant reduction to the quality of life.

The DCCT can be credited on focusing scientific research on the phenomenon of glucotoxicity. The kidneys, peripheral nerves, and the visual sensory system are composed of neuronal and endothelial cells that are insulin-independent, meaning that no hormone is required for uptake or metabolism of glucose thus making the tissues highly susceptible to glucotoxicity. The leading theories proposed to explain altered glucose metabolism are enhanced polyol activation, increased formation of advanced glycation end products (AGEs), and enhanced activation of oxidative phosphorylation. Although all the scenarios proposed have different mechanisms of how elevated glucose is deleterious, they share a unifying theme of glucose-induced oxidative stress.

Polyol Pathway

Polyol pathway hyperactivity is thought to produce hyperglycemic-induced oxidative stress. The polyol pathway may induce oxidative stress by lowering the amount of reduced glutathione (GSH), an important intracellular and extracellular anti-oxidant [10]. Excess glucose that has not been committed for oxidation to the Tricarboxylic Acid cycle (TCA cycle) is converted to sorbitol then fructose, a useful reaction since no energy input is required. In diabetics excess intracellular glucose gets oxidized to sorbitol by aldose reductase (AR), but at the expense of depleting NADPH, a co-factor that is also essential for the conversion of oxidized glutathione (GSSH) to GSH via glutathione reductase (Fig. 1). There are many studies suggesting that the polyol pathway is the major source of oxidative stress. Researchers have used a combination

of AR inhibitors (fidarestat®, epalrestat®) or AR knockouts animal models to support that the exaggerated flux through the polyol pathway leads to glucose-induced oxidative stress. For instance, a recent study by Ho *et al.* communicated the use of a combination of $AR^{-/-}$ and $AR^{+/+}$ mice, and a AR inhibitor (ARI) to study the extent the increased flux through the polyol pathway may lead to diabetic neuropathy. The researchers found that in streptozotocin (STZ) induced diabetes $AR^{+/+}$ mice had increased sorbitol and superoxide (O_2^-) levels and decreased GSH in the sciatic nerve in comparison to $AR^{-/-}$ mice [11]. Moreover, Ho and colleagues report that administering fidarestat® protected $AR^{+/+}$ mice from a reduction of motor and sensory nerve conduction velocities and diabetes-induced nerve fiber loss [11]. The research communicated by Ho *et al.* suggests that indeed the polyol pathway may in-fact play a significant role in glucose-induced oxidative stress, although throughout their studies they failed to show the expression levels of AR in AR-deficient mice. There are many excellent monoclonal and polyclonal antibodies against various isoforms of AR that would have been helpful to agree with their findings in AR knockout mouse models. Also, the use of ARI inhibitors is controversial because of concerns of safety, drawbacks of selectivity, and specificity [12]. In summary, although the polyol pathway may contribute to secondary complications of diabetes, there are many controversies surrounding the *extent* AR may play in glucose-induced oxidative stress.

Advanced Glycation End Products (AGEs)

AGEs are formed by the non-enzymatic reaction between the ketone or aldehyde groups of the glucose molecule and the amino groups of proteins [13]. The modification of proteins by AGEs is largely dependent on the intracellular concentration of glucose and whether the glucose molecule has been chemically modified. Research has shown that in diabetes mellitus the accumulation of AGEs is accelerated and activates the receptor of AGEs (RAGE) that may lead to the intracellular generation of ROS [14]. Ligand-induced activation of RAGE generates ROS predominately by NADPH oxidase and causes downstream activation of redox-sensitive transcription factors such as nuclear factor-kB (NF-kB) and vascular endothelial growth factor (VEGF) [13] (Figure 2). Although most work done on the AGE-RAGE axis is based on endothelial cells, i.e., how angiogenesis is promoted via the AGE ligand in diabetic models, the pathological effect of glycated proteins is also applicable to a heterogeneous population of cell types within a tissue [15, 16]. Presently there are various on-going clinical trials aimed at the pharmacological inhibition of AGEs formation, blockade of the AGE-RAGE interaction, and suppression of RAGE downstream pathways. For instance, Pimagedine® an inhibitor of AGE formation has proven efficacious in clinical trials because patients receiving the therapeutic had a slowed rate of progression to retinopathy [17]. Pyridorin® another pharmacological agent blocking AGE formation has had positive clinical outcomes because serum creatinine, a marker of nephropathy, was significantly decreased in patients receiving the therapeutic compared to those receiving placebo

[18]. A rather interesting clinical study found that by administering a recombinant soluble form of RAGE (sRAGE), consisting of the extracellular ligand binding domain, depressed the development of atherosclerosis and also ameliorated neuronal dysfunction [19]. All in all, pharmacologic studies aimed at AGE-RAGE axis intervention is a promising area of investigation suggesting that glucose-induced formation of glycated proteins, subsequent activation of RAGE, and ROS elevation may play a prominent role in the development of secondary complications in diabetes.

Increased Flux of NADH and $FADH_2$ to Oxidative Phosphorylation

Glucose may be converted to fructose in the polyol pathway or participate in the glycation of proteins through the Maillard process. However, the most significant role for glucose is oxidation through the TCA cycle. Hexokinase, the enzyme that converts glucose to glucose-6-phosphate, has a strong affinity for the carbohydrate and commits it solely for glycolysis [20]. Oxidation of glucose-6-phosphate in the cytosol produces pyruvate that is then shuttled into the mitochondrion. Mitochondria contain highly specialized enzymes (proteins) to convert the oxidized carbohydrate to energy in the form of ATP. The overall products of the TCA cycle are 6 equivalents of NADH and 2 equivalents of $FADH_2$ that are transferred to the inner mitochondrial membrane for oxidative phosphorylation [21]. The e^- transport chain is equipped with Complex I-IV that oxidize NADH and $FADH_2$ by transferring electrons through the inner mitochondrial membrane complexes and generating a proton gradient, an

essential electrochemical potential difference required to power Complex V and generate ATP [21]. Brownlee was the first researcher to suggest that in insulin-irresponsive tissues an increased intracellular flux of glucose induces the generation of elevated levels of reducing equivalents and produces a high electrochemical potential difference. The abnormally high proton gradient slows the transfer of e^- through Complexes I-IV inducing the series of oxidation reactions to 'leak' electrons and reduce oxygen molecules generating O_2^- radicals [22]. Figure 3 illustrates hypothetically that prior to cytochrome c reductase (complex III), O_2^- generation may take place. Fortunately, the O_2^- radical is short lived because the mitochondrial resident manganese containing superoxide dismutase (MnSOD) quenches the radical to form oxygen and hydrogen peroxide [23]. Although in hyperglycemic states some O_2^- escapes the dismutase and may react with mitochondrial produced nitric oxide (NO) and form a more deleterious ROS, peroxinitrite ($ONOO^-$) [24, 25]. $ONOO^-$ is a highly reactive free radical that has been shown to cause the nitration of tyrosine residues in various proteins, lead to DNA damage, and initiate apoptosis [26]. Free radical induced mitochondrial apoptosis has been carefully characterized to occur through the opening of the high conductance permeability transition (PT) that initiates mitochondrial permeability transition (MPT), a process that involves the nonselective diffusion of solutes with molecular mass of 15 kD, i.e., cytochrome c (12 kD), to the cytoplasm, lead to inner mitochondrial membrane depolarization, and initiate the apoptotic cascade [27].

Polyol hyperactivity, formation of AGEs, and increased flux of reducing equivalents through oxidative phosphorylation are the main metabolic pathways addressing glucose-induced oxidative stress. The pathways are primarily studied in endothelial cells under hyperglycemic *in-vivo* or *in-vitro* models. Long-term diabetes milletus is the major risk factor leading to coronary artery disease (CAD) accounting for high rates of morbidity and mortality among diabetics [28]. Since endothelia make up major portions of the vasculature, scientific research has primarily focused on how hyperglycemia affects the metabolism, structure, and viability of the cells. Unfortunately vasculopathy is often accompanied with neuropathy which may lead to ulceration and eventually amputation of a lower extremity. A long standing enigma of DPN is to understand the pathological disturbances elevated glucose may have on peripheral axons, sensory neurons, and glial cells. The SCs are specialized glial cells found in the peripheral nervous system (PNS) that form the myelin sheath, a highly specialized structure that enwraps large caliber axons in a spiral manner [29]. Moreover, at regular intervals the myelin sheath reduces in diameter and forms the nodes of Ranvier, a site responsible for the clustering of Na^+ and K^+ ion channels that allows for the stable and rapid propagation of action potentials (APs) [30]. An impaired SC phenotype leads to altered axonal properties that affect axonal caliber size and degeneration, and glial demyelination that may lead to muscle atrophy and sensory dysfunction [31].

As discussed above SCs play a vital role in the PNS. An important question that we want to answer is what effect chronic hyperglycemic-induced oxidative stress may have on the SC proteome. Specifically, does glucose-induced generation of O_2^- alter the mitochondrial proteome in a time dependent manner that may lead to organelle dysfunction and eventual apoptosis? To answer the question we employed proteomics to readily quantify the expression of proteins. Stable isotope labeling of amino acids in cell culture (SILAC) is a relatively new laboratory technique that when used in conjunction with mass spectrometry has proven to be excessively precise. For instance, researchers interested in characterizing functional protein complexes through SILAC are able to pin-point the *exact* number of proteins involved in the complex [32]. For our purposes, we will employ SILAC as a high-throughput technique to monitor the expression levels of proteins of the mitochondria under two variables; time and hyperglycemia conditions.

Eight years ago Ong and colleagues described the simple and straightforward approach of SILAC [33]. Since then, researchers have modified SILAC for many quantitative proteomic studies. SILAC involves the culturing of one population of cells with a light isotope and the other cell population with a heavy isotope. For instance, in our proteomic studies we metabolically labelled the hyperglycemic SC proteome by adding $^{13}C_6$-Lysine ($^{13}C_6$-Lys) to the cell culture media that is free of essential amino acid lysine. The normoglycemic cell population contained the light ($^{12}C_6$-Lys) isotope. The natural occurring $^{13}C_6$ isotope is stable, nonradioactive, and

readily incorporates into a cell proteome within a minimum of 2 population doublings [34]. Another benefit of employing $^{13}C_6$-Lys is that the trypsin enzyme cleaves proteins at the C-terminal to lysine and arginine, both occurring at an equal frequency of 5%, therefore half of the tryptic peptides generated will be labeled with $^{13}C_6$-Lys [35]. Moreover, tryptic digestion also generates numerous peptides that are an ideal size and charge distribution for mass spectrometry [35]. Our 1:1 mixture ratio of $^{12}C_6$-Lys and $^{13}C_6$-Lys peptide fragments will be analyzed by a hybrid linear quadrupole ion trap Fourier transform ion cyclotron resonance tandem mass spectrometer (LTQ-FT MS/MS). LTQ-FT MS/MS provides the highest mass resolution, mass resolving power, mass accuracy, and sensitivity of all available mass spectrometric analytical techniques available [36]. Therefore we are confident that our proteomic studies employing SILAC will yield an accurate depiction of the temporal effect hyperglycemic-induced oxidative stress may have on the proteome of the SC mitochondria.

Materials & Methods

Tissue Culture and Treatment

Primary SCs were isolated from the sciatic nerve of three or four day old neo-natal rat pups. The excised sciatic nerve was digested with 1% trysin in 1% collegenase for 30 min at 37º C and triturated to obtain a single celled suspension. The cell suspension was cultured in individual Techno Plastic Products (TPP) culture dishes with a growth surface area of 60 cm^2 and cultured at a cell density of 2.0 x 10^5. The newly isolated SCs were treated with .1 μM cystosine-β-D-arabino-furanoside for three days to remove contaminating cells such as fibroblasts and cultured in complete Dubelco's Modified Eagles Medium (DMEM), 10 % fetal bovine serum (FBS), 100 U/mL penicillin, 100 μg/mL streptomycin, 2 μM forskolin, and 1 g/L of glucose (5.5 mM). Passage one to passage six were used to conduct all experiments. High glucose was mimicked in culture by adding 24.5 mM glucose to the basal glucose concentration of 5.5 mM.

SILAC

The incorporation of heavy lysine isotopes into the whole cell proteome culture has been described previously [33]. Briefly, we prepared 4 liter batches of DMEM deficient in L-arginine and L-lysine. Complete SILAC media contained 100 U/mL penicillin, 100 μg/mL streptomycin, 10% dialyzed FCS (dFCS, Altas Biologicals), 1 g/L glucose, 2 μM forskolin, $^{12}C_6$-Arg, $^{12}C_6$-Lys, or $^{13}C_6$-Lys. For the experiments

described, heavy lysine $^{13}C_6$-Lys (Cambridge Isotopes) and light $^{12}C_6$-Arg (Sigma Aldrich) was used to label the proteome of SCs under chronic hyperglycemic stress (K6R0). SCs cultured in basal glucose levels were incubated with $^{12}C_6$-Arg and $^{12}C_6$-Lys (Sigma Aldrich) (K0R0). Preliminary experiments determined that prior to inducing hyperglycemic stress, the SCs had to maintained in labeling medium at least 10 days to get > than 95% isotopic incorporation in the SCs proteome.

Organelle Enrichment

After SCs were subjected to chronic hyperglycemia, the cells were washed three times with ice cold 1X PBS, trypsinized, harvested, and centrifuged at 500 x g for 10 minutes. The cell pellet was resuspended in MIBA buffer [10 mM Tris-HCL pH 7.4, 1 mM EDTA, 0.2 mM D-mannitol, 0.05 M sucrose, 0.5 mM Na_3VO_4, 1 mM NaF] containing 1X protease inhibitor cocktail (Roche Applied Science). The resuspended cell pellet was homogenized with 40 to 50 strokes and satisfactory cellular membrane rupture was determined by microscopic observation of low counts of intact cells and a multitude of free floating nuclei. If the organelle enrichment was intended for mass spectrometric analysis, the protein concentration of the homogenate was determined by the Bradford Assay using the Bio-Rad Protein Assay dye. Lysates from the K6R0 and K0R0 SCs were prepared and mixed in a 1:1 protein ratio and the homogenate was centrifuged at 500 x g for 10 minutes to obtain a crude nuclear pellet and supernatant. The crude nuclear fraction was purified as described by Hwang *et. al* [37]. Briefly, the crude nuclear pellet was washed once with 5 mL of buffer B [20

mM HEPES-KOH (pH 7.5), 10 mM KCl, 1 mM EDTA, 1 mM DTT, 0.25 M sucrose, and 1X protease inhibitor cocktail], resuspended in 2.5 mL of buffer B and mixed with an equal volume of buffer C [20 mM HEPES-KOH (pH 7.5), 10 mM KCl, 1mM EDTA, 1 mM DTT, 2.3 M sucrose, and 1X protease inhibitor cocktail]. The buffer B and C mixture was layered over 5 mL of buffer C and spun in a SW 41 rotor at 50,000 x g for 90 minutes. The enriched nuclei pellet was washed once with 1 mL of buffer A [20 mM HEPES-KOH (pH 7.5), 10 mM KCl, 1 mM EDTA, 1 mM DTT, and 1X protease inhibitor], centrifuged at 12,000 x g for 10 minutes and the remaining pellet was resuspended in 100 μL of ddH2O and stored at -20°C until use. To obtain an enriched mitochondrial fraction the supernatant was spun at 8,000 x g for 10 minutes and a heavy mitochondria (HM) pellet was formed. For SOD activity and immunoblot analysis, satisfactory mitochondrial enrichment was obtained from the HM fraction. For mass spectrometric analysis purified mitochondria was prepared by setting up a discontinuous Nycodenz density gradient. A stock 50% w/v Nycodenz solution was made by dissolving the powder in 10 mM Tris-HCL (pH 7.4) and working Nycodenz solutions of 40%, 34%, 30%, 25%, 23% w/v were made by diluting 50% Nycodenz in a solution containing 10 mM Tris-HCL (pH 7.4), 1 mM EDTA, 0.25 M sucrose. The HM fraction was resuspended in 25% Nycodenz and all the other working Nycodenz solutions were carefully over laid on top of each other starting from the highest concentration at the bottom of a centrifuge tube and the lowest concentration at the top of the tube. After the gradient was set up, the samples were spun in a SW 41 rotor at 50,000 x g for 90 minutes. The purified mitochondria

were extracted at the 25% - 30% interface, diluted with MIBA buffer, concentrated by centrifugation at 10,000 x g for 10 minutes, resuspended in 100 µL of MIBA, and stored at -20°C until use. Lastly, the cytosolic fraction was obtained by collecting the supernatant after the 8,000 x g centrifugation and spinning it at 100,000 x g for 60 minutes in a TLA 100.3 rotor. Typically the protein concentration of the cytosolic fraction is dilute. To obtain a concentrated cytosolic fraction, the cytosolic sample was concentrated by centrifugation using an Amicon Ultra filter (10,000 nominal molecular weight limit) to a final volume of approximately 100 µL.

Protein Sample Preparation for Mass Spectrometry

Approximately 100 ug of protein from enriched mitochondria, nuclei, and cytoplasm were fractionated using a 10% SDS-PAGE gel (100 volts, 6 hours) on a PROTEAN II xi vertical electrophoresis cell (Bio-rad). The proteins were visualized with coomassie blue, the individual lanes were each cut into 12-15 sections, and placed in silanized 1.5 mL eppendorf microcentrifuge tubes. The gel sections were destained (100 mM ammonium bicarbonate in 50% acetonitrile), reduced (10 mM dithiothreitol at 55° C for 60 minutes), alkylated (55 mM iodoacetamide for 30 minutes, protected from light), washed (100 mM ammonium bicarbonate in 50 % acetonitrile), dehydrated (100 % acetonitrile) and allowed to air dry. To cleave the proteins into peptide fragments, the gel pieces were hydrated (25 mM ammonium bicarbonate, pH 7.5 containing 12.5 ng/µL Trypsin Gold) and digested overnight at 37°C. Peptide extraction was performed the following morning (5% formic acid in 100 mM

ammonium bicarbonate, 5% formic acid in 50% acetonitrile, 5% formate in 100% acetonitrile), the supernantants were pooled, and concentrated to 25-40 μL in a Speed Vac.

Mass Spectrometry, Protein Identification and Quantification

The SILAC concentrates were separated by reverse-phase high performance liquid chromatography (RP-HPLC) and the eluate was introduced into a hybrid linear quadrupole ion trap Fourier transform ion cyclotron resonance tandem mass spectrometer, LTQ-FT MS/MS (ThermoFinnigan). The completed mass spectrometry run yielded a fragmentation spectra of singly, doubly, and triply charged peptides. The peptides and proteins were initially identified through the Mascot search engine (v. 2. 1, Matrix Science) and confirmed by Scaffold Protein Identification software (v 2.0, Proteome Software). The result file from Mascot was imported to MSQuant to automate the calculation of the expression ratio of peptide pairs ($^{13}C_6$-Lys /$^{12}C_6$-Lys). In instances where one or two peptide fragments identified a protein, manual calculation of peptide pair expression ratios was necessary. Manual verification of expression ratios followed the acceptance criteria of a fully tryptic peptide ($^{12}C_6$-Lys, or $^{13}C_6$-Lys) to be at least seven amino acids in length, had a detected series of at least 4 consecutive y-ions or b-ions, and a Mascot ion score of 25 or greater at a mass deviation of less than 6 ppm (3 times the dispersion of the mass deviations). If multiple peptide fragments were quantified for a given protein, the overall protein expression ratio was reported as the average of all

peptide fragments quantified with a given standard deviation. Lastly, a threshold expression ratio of 1.3 indicating a statistically significant change was derived by averaging the expression ratio of all the peptides quantified at a given time point, calculating the respective standard deviation and multiplying it by three [38].

SDS-PAGE and Immunoblot Analysis

Three or eight micrograms of total protein of the subcellular fractions were separated in a 12% SDS-PAGE (100 volts for 90 minutes), transferred on to a nitrocellulose membrane (30 volts overnight), and immunoblotted for the proteins of interest. Blotting was performed by initially washing the nitrocellulose membrane three times, 20 minutes each with 5% dry milk in 1X PBST. The first step in detecting the protein of interest occurred by adding the primary antibody to 5% dry milk in 1X PBST and incubating for 2 hours at room temperature. After the primary antibody incubation, the nitrocellulose membrane was washed (3 times for 10 minutes) to remove unbound antibody then the secondary antibody was added to 5% dry milk in 1X PBST and incubated for one hour. Lastly, the nitrocellulose membrane was washed three times with 1X PBST for 5 minutes and protein detection occurred by adding a chemiluminescent reagent (GE Healthcare) that reacts with horse-radish peroxidase of the secondary antibody emitting a luminescent signal to allow detection by X-Ray film (MIDSCI).

Antibodies

Primary Antibodies: Anti-MnSOD (dilution 1:600, Upstate Biotechnology), anti-β-actin (dilution 1:3000, Santa Cruz Biotechnology), anti-prohibitin-1 (dilution 1:400, Neomarkers), anti-p62 nucleoporin (dilution 1:2500, BD Transduction Labs), anti-LDH (dilution 1:1000, Sigma-Aldrich), anti-GRP78 (dilution 1:500, Santa Cruz Biotechnology).

Secondary Antibodies: Goat-anti-rabbit IgG (dilution 1:5000), goat-anti-mouse IgG (dilution 1:5000), and anti-goat IgG (dilution 1:5000) were purchased from Santa Cruz Biotechnology.

Superoxide Dismutase (SOD) Activity Assay

To assess SOD activity indirectly, we followed the conversion of the water-soluble tetrazolium salt (WST-1) to WST-1 formazan, a proprietary compound from Dojindo Molecular Technologies. The assay was conducted by adding 0.5 to 3 micrograms of protein from the HM fraction of the control and treated samples and then adding a working concentration of WST solution. To generate O_2^-, XO was added to the sample, mixed thoroughly, incubated at 37ºC for 20 minutes, and the colorimetric conversion of WST-1 to WST-1 formazan was measured at a wavelength of 450 nm. The principal of the assay rest on the fact that the generation of O_2^- by XO and the rate of reduction of formazan by O_2^- is linear. Therefore, the generation of the formazan is dependent on the amount of MnSOD present in a particular sample.

Unless stated elsewhere, all samples including SOD standard (SOD from bovine erythrocytes, Sigma) and blank samples were run in triplicate in 96 well tissue culture test plates (TPP).

Superoxide Measurements

To assess real-time O_2^- generation in primary SCs, we used cell-permeable dyhroethidium (DHE), a fluorescent probe from Invitrogen. SCs were seeded at a density of 1.0 x 10^3 into 96 dark well tissue culture plates (Corning Inc.). At about 90% confluency, the SCs were exposed to acute and chronic episodes of hyperglycemia and then subject to the DHE assay. A stock concentration of 30 mM DHE was made by dissolving the powder in DMSO. A working concentration of 150 μM DHE was made by diluting the stock in HEPES-buffered saline solution [10 mM HEPES (pH 7.4), 150 mM NaCl, 5 mM KCl, 1 mM $MgCl_2$, 1.8 mM $CaCl_2$] and adding it directly to the culture media at a final concentration of 15 μM. The working concentration of the DHE solution was added 15 minutes prior to the termination of hyperglycemic episodes, media was removed, washed once with ddH_20 and fluorescence read immediately on the Biotek FL600. The ratio of ethidium (excitation: 530 nm, emission: 590 nm) over DHE (excitation: 485 nm, emission: 530 nm) was determined.

Knockdown MnSOD

Primary SCs were subject to shRNA mediated knockdown of the expression of MnSOD. Clone TRCN0000123391 (5'CCGGGAGGCTATCAAGCGTGACTTTCT CGAGAAAGTCACGCTTGATAGCCTCTTTTTG-3') purchased from Sigma Aldrich showed optimal silencing efficiency of MnSOD. The oligonucleotide sequence obtained from Sigma was ligated into a pLVX-shRNA vector and cotransfected with Lenti-X HT packaging mix (Clontech) into HEK 293 cells to produce shRNA lentivirus for infecting the SCs. After two days of cotransfection, the 293 cells were harvested to obtain stock lentivirus targeting MnSOD. The 293 cells were harvested by collecting the cell media and centrifuging at 250 x g for 10 minutes. The resulting supernatant was centrifuged at 50,000 x g for 60 minutes. The viral pellet was resuspended in 1 mL of medium (1% antibiotic, 10% FBS, 4.5 g/L glucose), aliquots prepared, and stored at -80° until use.

Results

Validation of Isotope Incorporation into the SC Proteome

To determine an approximate time frame needed to obtain full isotope incorporation into the SCs proteome, deuterated leucine (Leu-d3) was used. The use of Leu-d3 for preliminary experiments was warranted because it is a cheaper alternative to using $^{13}C_6$-Lys which has been used for SILAC. Primary SCs were incubated in complete DMEM deficient in leucine while Leu-d3 was added directly to the medium at a stock concentration of 10 mg/mL. Figure 4 depicts the time frame of Leu-d3 incorporation. At days 2 and 8, Leu-d3 is steadily accumulating in the SC proteome while unlabeled leucine detection is diminishing. By day 10, virtually all of the peptides containing unlabeled leucine have been replaced, while peptides synthesized with Leu-d3 accumulate in the proteome due to cell mitosis and protein turnover. From the results of Figure 4, we determined that primary SCs must be incubated with the isotope label for approximately 10 days or 5 to 6 population doublings to achieve a level of 95% isotopic incorporation which is acceptable for SILAC.

Figure 5 illustrates the schematic for examining the temporal effect of hyperglycemic stress on the SC proteome. Two cell populations were cultured concurrently, cells incubated with basal glucose concentration (5.5 mM) received $^{12}C_6$-Lys and cells subjected to hyperglycemia (30 mM glucose) were cultured with $^{13}C_6$-Lys. After allowing sufficient time for isotope incorporation, one set of cells remained with 5.5

mM glucose and the other set of cells were incubated with 30 mM of glucose for 2, 6, and 16 days of hyperglycemic stress. The use of $^{13}C_6$-Lys is ideal for proteomic experiments because following tryptic digestion many peptides possess a C-terminal Lys. Moreover, the physicochemical properties of $^{13}C_6$-Lys are not altered significantly in relation to $^{12}C_6$-Lys which allows for perfect coelution from a chromatography column[35]. Equal elution time for $^{12}C_6$-Lys and $^{13}C_6$-Lys greatly simplifies mass spectrometric experiments aimed at determining protein expression ratios of basal and hyperglycemic cell populations.

Assessment of Organelle Enrichment

The central aim of the research was to compile data to make an unbiased assessment of the effect chronic hyperglycemia and subsequent O_2^- generation may have on the mitochondrial proteome. To achieve this end, it was necessary to enrich mitochondria by density gradient centrifugation as discussed in the materials and methods section. Enriched nuclei and cytosolic fractions were also obtained to make a comparative study of the relative change hyperglycemia introduces into the proteomes among the three subcellular fractions. Figure 6 shows organelle enrichment using established marker proteins for various organelles. For instance, anti-MnSOD was used to detect the mitochondrial resident dismutase that resides specifically in the mitochondrial matrix and intermembrane space and can be used as a marker for mitochondrial purity. The result suggests a purified mitochondrial fraction compared to the crude HM fraction at the correct mass weight of 24 kDa for

the dismutase. A rigorous test of organelle enrichment must entail more than one marker for purity, therefore a prohibitin-1 antibody was also used. Prohibitin-1 is a mitochondrial resident chaperone involved in the essential functions of stabilizing, folding, and refolding newly synthesized or misfolded proteins [39]. From the results of Fig. 6, again the purified mitochondria fraction is more enriched than the crude mitochondrial fraction, namely the HM. Nuclei enrichment was also determined by blotting for nucleoporin (p62), a 62 kDa protein that makes up part of the nuclear pore complex, an essential nuclear structure regulating the flow of macromolecules between the nucleus and cytoplasm [40]. The blot for p62 demonstrates that our method to enrich nuclei is satisfactory since the other four fractions do not show a trace of the nuclear pore protein. The third fraction obtained was the cytosolic fraction, in which the lactate dehydrogenase (LDH) marker was used to assess for enrichment by detecting the cytosolic and plasma membrane associated protein. LDH is a 35 kDa protein that plays a critical role in anaerobic conditions by converting pyruvate to lactic acid [41]. Lastly, glucose-regulated protein (GRP78) antibody was used to detect endoplasmic reticulum (ER) contamination. GRP78, a 78 kDa protein, is a typical ER marker since it plays a central role in homeostasis such as binding misfolded proteins and ER Ca_2^+ binding [42]. The GRP78 blot show that all the fractions contain some level of ER proteins which suggests that purification of the ER from other organelles is difficult. Nevertheless, when we obtained our peptide sequences from mass spectrometry we were able to collate proteins belonging to the organelle of interest by their gene ontology annotation. For instance, the percentage

of ER proteins found in nuclear, mitochondrial, and cytosolic fractions were 14.7%, 22.7%, 0.7%, respectively, a substantial low percentage of the total proteins identified belonging to the particular fraction.

Distinct Effects of Hyperglycemia on Enriched Subcellular Fractions

In the introduction we discussed that excess glucose may lead to the generation of increased levels of O_2^-. Specifically, the aim of the SILAC experiments was to assess protein expression level changes in chronic hyperglycemic conditions that may be due to oxidative stress. A total of 317, 332, and 432 proteins were identified and quantified in enriched mitochondria, nuclear, and cytoplasmic fractions respectively. The expression ratio versus protein number was plotted for each protein of the three fractions to readily observe the changes graphically (Fig. 7). Of the mitochondrial proteins, days 2 and 6 of hyperglycemic stress proved to introduce the most statistically significant increase in expression changes; 90% of the proteins quantified had a ratio greater than 1.3 (Figure 7a). Interestingly, at day 16 only 56% of the mitochondrial proteins showed a fold increase of 1.3.

The nuclear fraction also seemed to be affected by chronic hyperglycemia since 60% and 54% of the nuclear proteins quantified for days 2 and 16 had a statistically significant increase in their expression ratios (Fig. 7b). Cytosolic proteins were the *least* affected by the various periods of glycemic stress. For instance, after 2 and 6

days of 30 mM glucose, 91.7% and 84% of the proteins quantified failed to show a statistically significant shift of an expression ratio (Firg. 7c).

Since the graphical observation of the expression ratio can only yield a generalization of the effect of chronic hyperglycemic stress, we next categorized the nuclear proteins into functional classes to better understand which proteins are affected by high glucose conditions. The proteins were clustered by their roles in chromatin regulation, mRNA splicing, RNA binding, and transcriptional regulation. The data in figure 8 suggests that proteins involved in chromatin regulation may be affected by hyperglycemic-induced oxidative stress at 2 and 16 days because their increased expression ratios were statistically significant. Researchers in the genotoxicity field have shown that H_2O_2, a by-product of the dismutation of O_2^-, induces nuclear chromatin degradation in oligodendrocytes so the overexpression we observed may be reparative [43, 44]. Since glucotoxicity has been firmly established, chronic hyperglycemia may be adversely affecting the SC proteome [45]. Proteins involved in transcription regulation, mRNA splicing, and RNA binding were statistically significantly overexpressed at days 2 and 16 which may suggest an increase in protein turnover due to hyperglycemic stress.

Similarly, the mitochondrial proteins were clustered into functional classes. The proteins were grouped into major mitochondrial roles such as TCA cycle, transport, chaperone activity, detoxification, fatty acid metabolism, and metabolism (Fig. 9).

All of the proteins clustered into functional classes had a statistically significant increased expression ratio for days 2 and 6. Notably, the TCA and detoxification proteins at day 6 had a pronounced increased in their expression ratio that was statistically different from 2 days of hyperglycemia. In contrast, a statistically significant decrease for all functional classes was observed for day 16 proteins when compared against days 2 and 6.

The mitochondrion is the primary site of glucose metabolism. Therefore, it is reasonable to observe an average 1.54 fold increase in the expression ratio of enzymes involved in the oxidation of glucose. For instance, excess glucose will inevitably generate a slew of reducing equivalents (NADH and $FADH_2$) from the TCA cycle. To presumably accommodate the increase flux of reducing equivalents the components of the electron transport chain involved in oxidative phosphorylation must be increased. Indeed after 2 and 6 days of hyperglycemic stress, complexes I through V showed an increase in expression ratios (Fig. 10). In conjunction with a significant overexpression ratio of TCA proteins and components of the respiratory chain, detoxification proteins also exhibited higher expression ratios from days 2 to 6 (Fig. 9). As discussed in the introduction, Brownlee and colleagues were the first to propose that excess glucose may lead to the generation of toxic overproduction of O_2^- [22]. The major O_2^- scavenger residing in the mitochondria is MnSOD, which had an average expression ratio of 1.8 at days 2 and 6. Similar to the trend exhibited for proteins quantified for day 16, the expression ratio decreased to 1.4 for MnSOD.

Other notable detoxification enzymes that exhibited similar increases in overexpression under chronic hyperglycemic stress were Park7 (DJ-1) and Prohibitin-1. Prohibitin-1 has been implicated to play a part in mitochondrial function and research has shown that knockdown of the protein can increase oxidative stress [46]. The expression ratio of prohibitin-1 under chronic hyperglycemia was 1.4 in which a confirmatory immunoblot further supports the mass spectra findings (Fig. 11a.). The other detoxification protein that had a statistically significant increased expression ratio was DJ-1, a novel protein in which loss-of-function mutation is thought to cause autosomal recessive early-onset Parkinsonism [47]. Moreover, work by Canet-Aviles *et al.* has show that oxidative stress conditions induces the translocation of DJ-1 from cytosolic pools to the mitochondrion [48]. Similarly results in figure 11b show the accumulation of DJ-1 in the HM fraction by hyperglycemia. Figure 11c illustrates the mass spectra of cytosolic and mitochondrial DJ-1, with an expression ratio of 1.1 and 1.8 respectively, two ratios that statistically differ ($p < .05$). Together, these results support that the SC proteome may counter hyperglycemic-induced oxidative stress by overexpressing detoxification proteins to safeguard the integrity of oxidative phosphorylation enzymes, nuclear transcription proteins, and cell viability in general.

Increased Expression of Manganese Containing SOD

MnSOD is the primary dismutase to counter oxidative stress in the mitochondrion [49]. Figure 12 shows the mass spectra of a peptide fragment of MnSOD and Cu/Zn SOD enzymes. A general comparison of figures 12a and 12b reveals that 30 mM

glucose induced an overexpression of MnSOD enzyme, while the cytosolic O_2^- scavenger Cu/Zn SOD does not increase in expression. Specifically, figure 12a depicts the spectra for a peptide fragment of MnSOD with an average expression ratio of 1.8 for days 2 and 6 of hyperglycemic stress. In contrast, figure 12b depicts a peptide sequence for the Cu/Zn SOD enzyme with a statistically insignificant change of expression ratio, namely an average ratio of 1.0 for 2, 6, and 16 days of hyperglycemia. To confirm the data obtained from mass spectrometric analysis, we performed independent experiments and measured the expression ratio of both the mitochondrial and cytosolic dismutases by traditional immunoblot analysis. The confirmatory experiments used standard DMEM media (10% FBS, 1% penicillin-streptomycin solution, and 1 g/L of glucose) instead of the SILAC media described in the materials and methods section. Figure 13a shows a representative blot of the HM fraction of primary SCs incubated with 30 mM glucose for 2, 4, 6, and 16 days. Clearly, hyperglycemia is inducing an increase in the expression of MnSOD. Figure 13b shows a densitometric analysis of three experiments for days 2, 4, and 6 days of glycemic stress. In figure 13d we were able to confirm that cytosolic Cu/Zn SOD does not increase under chronic hyperglycemia in line with the results obtained by mass spectrometry. Typically an observed overexpression of MnSOD must correlate with an increased enzymatic activity and results in figure 13c show the indirect measure of MnSOD activity. The HM fraction was used to assess the dismutase activity of the various cell lysates and show that 6 days of hyperglycemia induced an

increase in MnSOD activity that is statistically different from the other time points of hyperglycemia.

Lack of Increase O_2^- Levels in Hyperglycemic States

Various researchers have published reports implicating a cause and effect relationship between elevated glucose levels and oxidative stress in cell types such as dorsal root ganglion (DRGs) sensory neurons, endothelial and pancreatic β cells [50-52]. Therefore, we set out to determine whether the observed phenomenon in the above described cells can be replicated in primary SCs. Moreover, we have shown earlier that in the mitochondrial proteome there is an overexpression of MnSOD under glycemic stress which may be induced by elevated O_2^-. Before we began to assay for O_2^- in glycemic stressed cells, we used H_2O_2 to confirm that we can measure the oxygen free radical. Within a 15 minute incubation period, the free radical generator induced an increase in O_2^- levels (Fig. 14a). Vincent and colleagues determined that acute hyperglycemic conditions led to oxidative stress in DRGs [50]. In primary SCs, acute hyperglycemia did not generate any significant increases in the free radical. Figure 14b shows the results of three independent experiments, where SCs were stressed for 4 and 6 hrs with 30 mM glucose and immediately assayed for O_2^-. The results of figure 14b suggest that in primary SCs acute hyperglycemia does not lead to oxidative stress. The mass spectrometric experiments were conducted in chronic hyperglycemic conditions, where we showed that 2 and 6 days of elevated glucose led to a significant overexpression of detoxification proteins. Therefore, prolonged

periods of hyperglycemia may be the required factor to record elevated O_2^- levels. Unfortunately, figure 14c. shows that chronic hyperglycemia also did not generate significant amounts of the oxygen radical. The results of figure 14 suggest that acute and chronic glycemic stress does not lead to generation O_2^- in primary SCs. More importantly, the observed proteomic changes in the various subcellular fractions leads us to speculate that the changes are independent of oxidative stress, specifically O_2^-.

MnSOD Knockdown and Reassessment of O_2^- Levels in Hyperglycemic States

Mass spectrometric and immunoblot data suggest that chronic hyperglycemia induces an overexpression of protective proteins and enzymes to prevent glucose toxicity. As discussed in the introduction, glucose-induced oxidative stress may lead to mitochondrial membrane depolarization, activation of the mitochondrial permeability transition which causes the non-selective diffusion of solutes less than 15 kDa out to the cytoplasm, particularly cytochrome c, ultimately activating caspases and initiating apoptosis [27]. To prevent ROS-induced apoptosis in primary SCs, our data suggests that chronic hyperglycemia causes the overexpression of detoxification enzymes (proteins) which may be sufficient to quench O_2^- levels explaining why we did not see a significant increase of ROS levels. Therefore our next approach was to employ shRNA to knockdown MnSOD in SCs and measure O_2^- levels to determine whether the oxygen free radical can contribute to altering the SC proteome. Figure 15a shows a reduction of MnSOD expression in the HM fraction of primary SCs infected with a lentivirus containing shRNA with a complementary sequence to mRNA of MnSOD.

The same HM fraction was also subject to SOD activity measurements and clearly the reduced expression level of MnSOD correlates with a statistically significant reduction of activity (Fig. 15b). After validating that our shRNA sequence against MnSOD efficiently knockdowns the enzyme, we repeated our acute and chronic hyperglycemic experiments after 2 days of lentivirus infection. In figure 16a we measured O_2^- levels after 4 hours of hyperglycemic stress with various dilutions of the lentiviral stock. The acutely stressed SCs shows that stronger knockdown of the MnSOD did not alter the levels of O_2^-. Similarly, SC were incubated with various lentiviral dilutions and stressed for 2 days of hyperglycemia. The data in figure 16b suggests that after knockdown of MnSOD and chronic hyperglycemia are not sufficient variables to alter the oxidative status of SCs. Moreover, stressing the SC with 120 μM H_20_2 for 15 minutes caused a slight increase in O_2^- generation (Fig. 16b.). Next, we knocked down MnSOD and stressed the SCs with 120 μM H_20_2 and noticed a substantial increase in the generation of O_2^- (Fig. 16c.). Overall, the data presented in figure 16 allows a comparison between 30 mM glucose and H_2O_2 suggesting that the carbohydrate is not a significant generator of O_2^-.

Discussion

Throughout the studies presented in this body of work, the data generated suggests that SCs are surprisingly resilient to high glucose stress. It is important to consider that SCs play a prominent role in the nerve. Earlier we discussed that SCs are highly specialized glial cells that collectively form the myelin sheath and nodes of Ravier providing a significant increase in nerve impulse conduction. Moreover, the active uptake and oxidation of glucose is not modulated by insulin, but rather by axonal energy demands [53]. Therefore, axons that are continuously firing action potentials require more ATP, thus more glucose oxidation, to *actively* regulate the fluctuating concentrations of Na^+ and K^+ ions. Since SCs enwrap the axons, they serve yet another purpose of regulating the flow of glucose levels [54]. Fluctuating low and high concentrations of glucose that transverse the SCs may serve as an evolutionary trigger affording protection to itself and the axon.

SILAC and mass spectrometry allowed the high-throughput protein quantification and temporal assessment of the effect high glucose had in three major subcellular fractions. We were able to determine the expression levels of over 300 proteins in the mitochondrial, nuclear, and cytosolic fractions. A statistically significant increase in protein expression was observed for 2 and 6 days in mitochondrial proteins, while nuclear proteins were significantly overexpressed at days 2 and 16. Grouping the

mitochondrial and nuclear proteins into functional classes revealed a clearer picture of the effect hyperglycemia may have on the SC proteome. Specifically, high glucose induced mitochondrial proteins important in detoxification, TCA cycle, and oxidative phosphorylation to be overexpressed. Moreover, we conducted independent chronic hyperglycemic experiments and immunoblotted for MnSOD, prohibitin-1, and DJ-1. The proteins mentioned above serve vital anti-oxidant and anti-apoptotic functions under cellular stress, which were consistently overexpressed in the proteomic studies and confirmatory immunoblots. After clustering the nuclear proteome by function we observed a statistical overexpression of proteins involved in transcriptional regulation, mRNA splicing, and RNA binding. The results of the two subcellular compartments suggest that chronic hyperglycemia is indeed affecting the SC proteome. Brownlee was the first to propose that hyperglycemia may induce oxidative stress, specifically O_2^-. Therefore, our proteomic conclusions were initially centered under the idea that oxidative stress was inducing the observed protein level changes. Although, an exhaustive pursuit of O_2^- generation through a multitude of acute and chronic hyperglycemic experiments, subsequent knockdown of MnSOD, then repeated O_2^- measurements revealed that glucose did not generate a significant rise in the oxidant. It may be likely that enzymes such as GSH, mitochondrial translocation of DJ-1, and Cu/Zn SOD may play a synergistic effect to help evade oxidative stress imposed by a decreased expression of MnSOD. Earlier we discussed that O_2^- may react with NO to form $ONOO^-$ thus cause the nitration of tyrosine residues of proteins [26]. The enriched subcellular fractions were also probed for

nitrotyrosine without any success. The data gathered in these experiments suggests that although altered glucose metabolism does cause the overexpression of proteins in the nuclear and mitochondrial fraction, the effect is independent of the O_2^- radical. Hyperglycemia induces an intracellular protective response that may be evolutionarily selected due to the protective role SCs serve in the nerve.

In the introduction we mentioned that most hyperglycemic-induced oxidative research is studied on endothelial cells since diabetes is predominantly a cardiovascular disease causing CAD, peripheral arterial disease (PAD), and microvascular damage. There are a multitude of studies showing glucose-induced generation of O_2^-, $ONOO^-$, endothelial dysfunction and eventual apoptosis [55-57]. In contrast, our studies employing SCs to measure glucose-induced oxidative stress is one of kind. To reiterate, our studies yielded conclusions that support the idea that SCs may serve a protective role under hyperglycemic stress, since they have a built in mechanism that is activated to counter a high and low influx of glucose. For instance, in our proteomic analysis we observed an overexpression of various peptides of the mitochondrial resident MnSOD. Immunoblot analysis of chronic hyperglycemic SCs also suggested that MnSOD is overexpressed in a time dependent manner. The overexpressed dismutase correlated with an increase in activity of the enzyme, that was indirectly measured by following the colorimetric conversion of WST-1 to WST-1 formazan. In contrast, there are no studies published suggesting that endothelial cells overexpress or downregulate detoxification proteins to protect from a high

influx of glucose. Therefore, the glucose-induced oxidative stress theory may in fact be more relevant in endothelial cells than SCs.

Future Directions

To solidify our conclusion suggesting that SCs are protective even under hyperglycemic stress, a series of experiments need to be executed. For instance, we would measure apoptosis between normoglycemic and hyperglycemic cells to determine whether there is a significant difference in cell death. There are many assays available that give a fairly accurate measure of apoptosis, such as measuring oligonucleosomal DNA fragmentation and performing Caspase-3 assays. If in fact the overexpression of protective proteins is affording protection to the mitochondria specifically, then it would be interesting to measure the rate of ATP production between basal and high glucose cells. If the protective mechanisms are activated in hyperglycemic stressed SCs, the SCs should not decline significantly away from normoglycemic SCs in terms of energy production. The measure of apoptosis and ATP production would be firm indicators of fairly healthy SCs in high glucose cell culture conditions.

In vitro observations do not necessarily translate to similar results *in vivo*. The proteomic data we obtained from hyperglycemic SCs cell cultures would need to be carried out in mouse models to determine if the same results apply. Kruger and colleagues have recently described the technique of developing a SILAC mouse where they fed mice with a heavy diet, e.i., $^{13}C_6$-Lys food pellets, for over four

generations and noticed complete label in all organs tested in the F2 generation [58]. The SILAC mouse approach can yield data that may be more relevant to human diabetic patients in comparison to cell culture models.

Figures

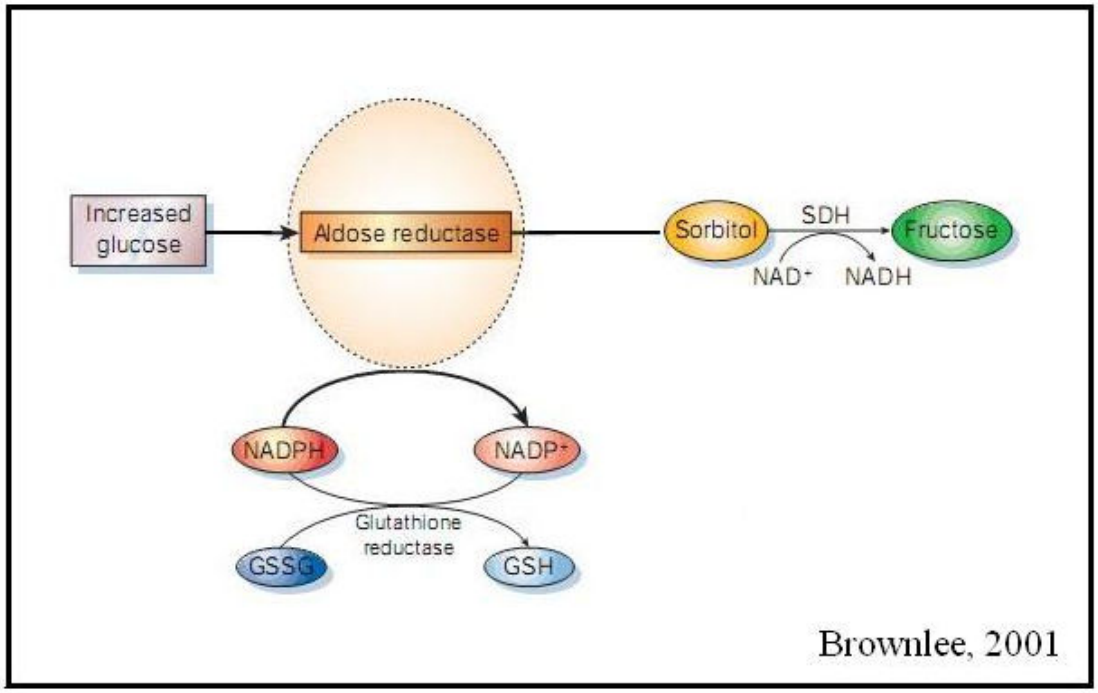

Figure 1. Polyol Pathway Hyperactivity Reduces Levels of GSH.
Glucose that is not chemically altered by hexokinase is free to function as a substrate for aldose reductase (AR). AR converts glucose to sorbitol and through sorbitol dehydrogenase (SDH) fructose is formed, a reaction that does consume ATP generating more energy for glycolysis and glyconeogenesis. In hyperglycemic states, it is hypothesized that polyol pathway hyperactivity reduces the levels of NAPDH, a cofactor essential for glutathione reductase (GSH) to reduce GSSH from the oxidixed form.

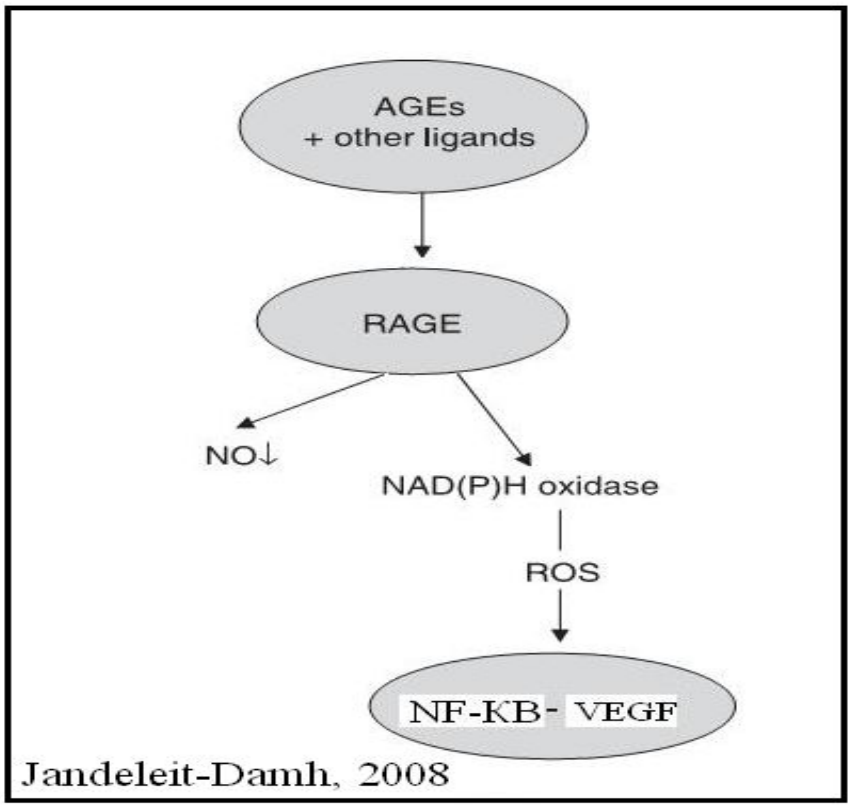

Figure 2. Formation of AGEs Increases ROS and Activates Redox-Sensitive Transcription Factors. The non-enzymatic addition of glucose to proteins forms advanced glycation end products (AGEs) that along with other ligands activates RAGE. It has been shown that RAGE activation leads to decreased NO and increase activation of NADPH oxidase, an enzyme that generates O_2^-. Redox-sensitive transcription factors are activated by ROS, e.i., VEGF activation promotes angiogenesis [59].

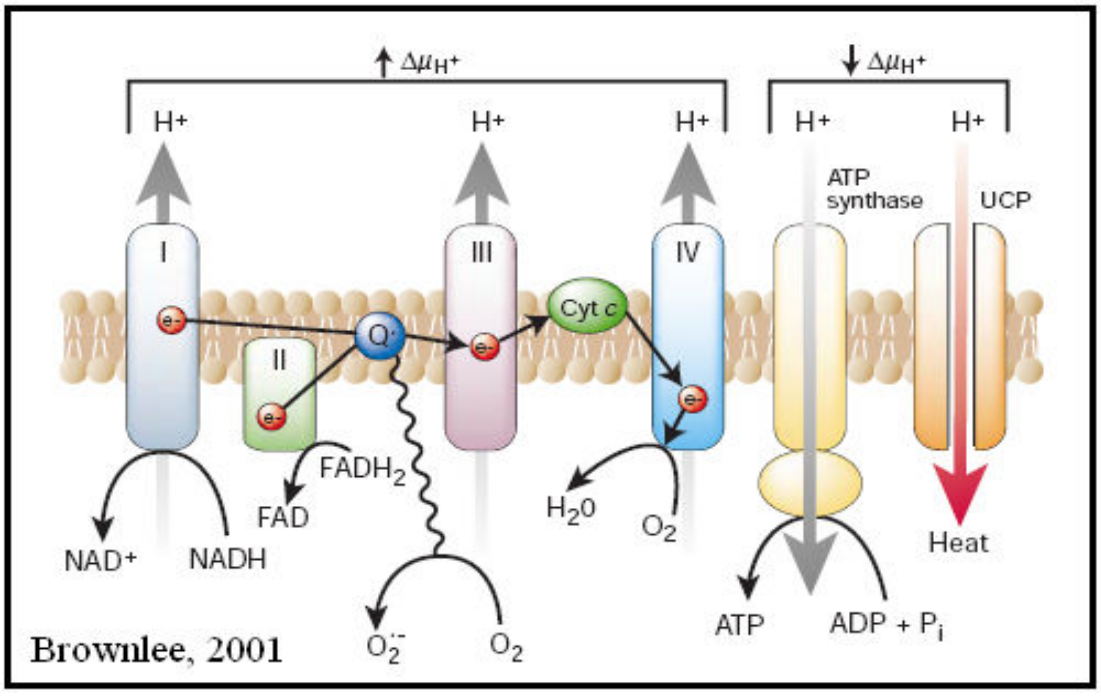

Figure 3. Enhanced Oxidative Phosphorylation and O_2^- Generation.
The oxidation of glucose through the TCA cycle generates reducing equivalents (NADH and $FADH_2$) that are shuttled to the inner mitochondrial membrane and through e^- transfer through complex I-IV generate a proton gradient to power complex V (ATP synthase) and produce ATP. In hyperglycemia, the TCA cycle produces excess reducing equivalents generating a high electrochemical potential difference leading to a slowed transfer of e^- through complex I-IV causing the leakage of electrons and reducing O_2 to O_2^-.

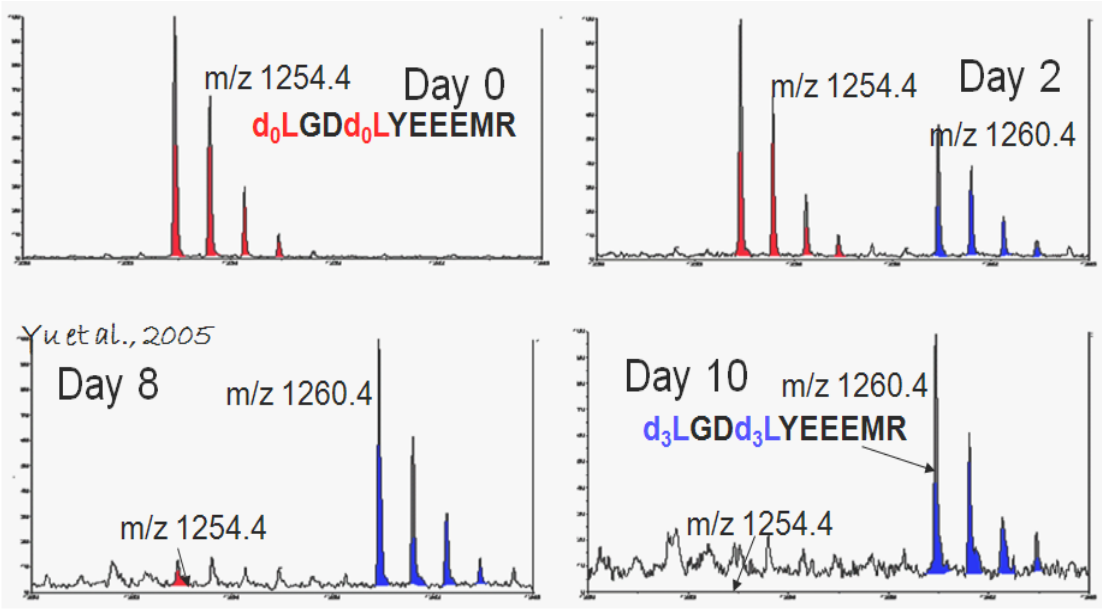

Figure 4. Isotopic Incorporation into The SC Proteome.
At day zero Leu-d0 is the prominent ion peak observed in the mass spectra. After prolonging the time of incubation with Leu-d3, there is a mass shift from 1254.4 to 1260.4, indicating that the SC proteome is replacing the unlabeled Leu. By day 10, peptides containing Leu-d0 are virtually undetectable while peptide fragments containing isotopically-enriched Leu-d3 emit the strongest ionization peaks.

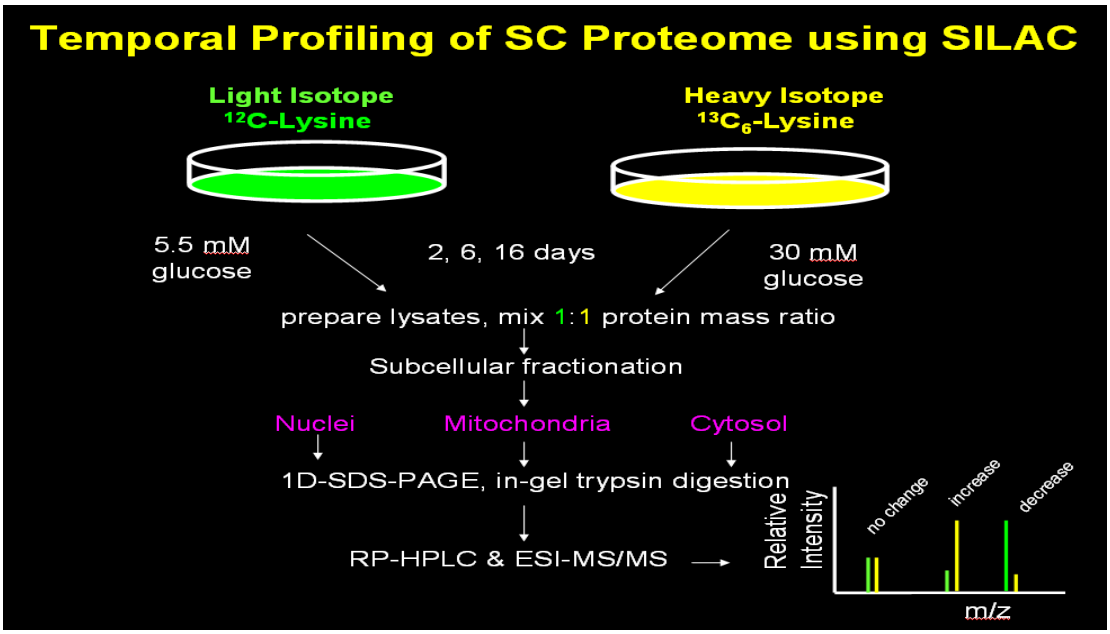

Figure 5. Schematic for Chronic Hyperglycemic Experiments Utilizing SILAC. The flow chart depicts the SILAC workflow to assess whether hyperglycemic conditions are altering the SC proteome. To determine the expression ratio between the light and heavy isotopic-labeled cells, the crucial step in the schematic is mixing the lysates in a 1:1 ratio. We obtained three enriched subcellular fractions by differential centrifugation, separated the proteins on SDS-PAGE, ran the concentrates in a mass spectrometer, and quantified the relative intensity of light and heavy peptides throughout 2, 6, and 16 days of hyperglycemic stress.

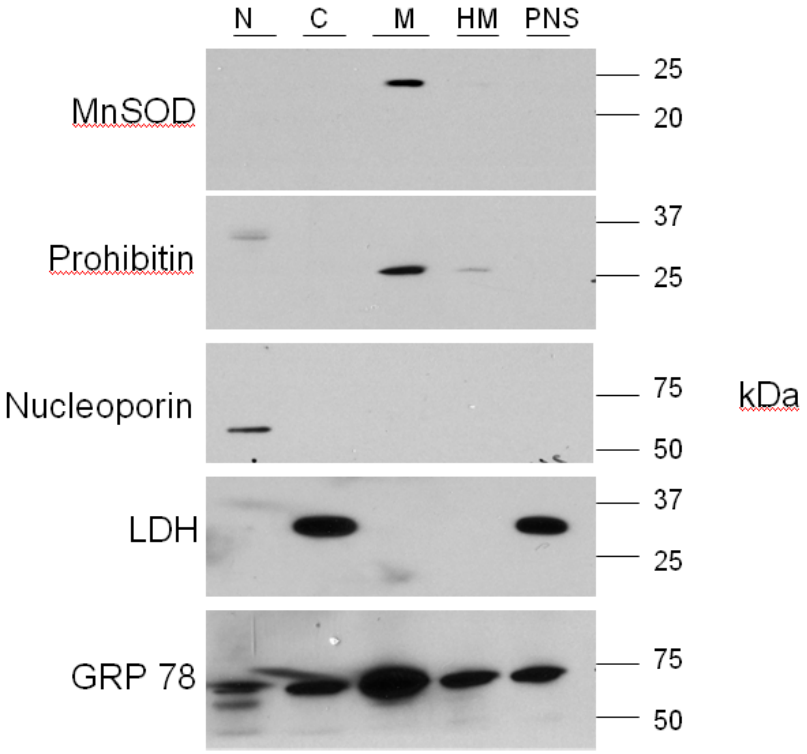

Figure 6. Assessment of Organelle Enrichment.
The figure depicts a series of immunoblots analyzing the degree of enrichment of nuclei, mitochondria, and cytoplasmic proteins. Anti-MnSOD (24 kDa) and anti-prohibitin-1 (28 kDa) were used to assess the levels of mitochondrial enrichment. Anti-nucleoporin (62 kDa) was used as a marker for enriched nuclei. Anti-LDH (35 kDa) was used as a marker for cytoplasmic protein enrichment. GRP78 (78 kDa), a marker for ER and microsomes, contaminated all the subcellular fractions to various degrees. Protein organelle discrimination occurred by gene ontology annotation. Nuclear fraction (N), cytoplasmic fraction (C), purified mitochondria (M), heavy mitochondria fraction (HM), and post-nuclear supernatant (PNS).

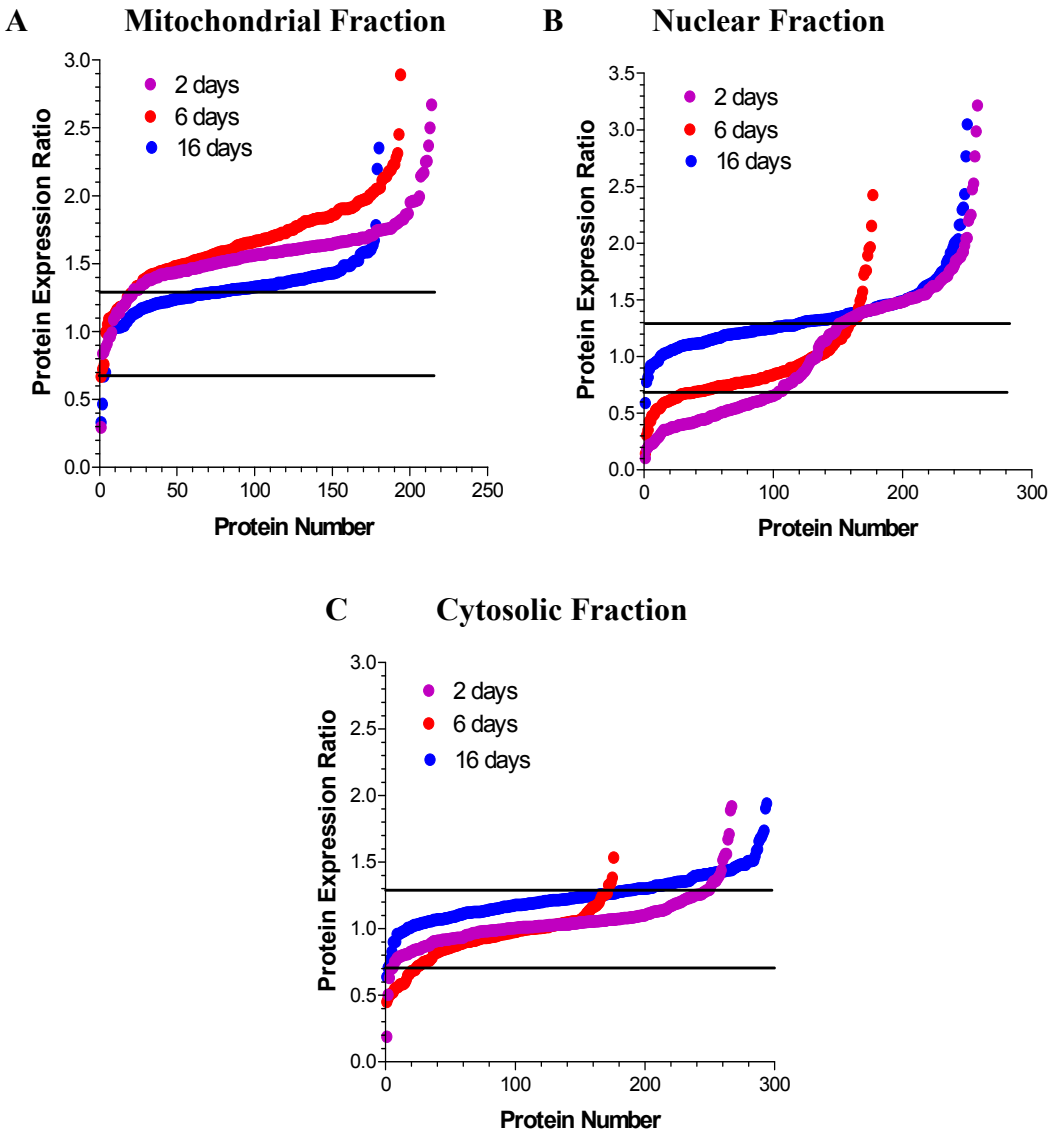

Figure 7. Variable Response of Glycemic Stress on Three Subcellular Fractions. 30mM glucose was added to $^{13}C_6$-Lys cells for 2, 6, and 16 days and compared to control $^{12}C_6$-Lys cells. **(A)** Purified mitochondrial proteins at days 2 and 6 showed the highest increase in their expression ratio, about 90% of the proteins showed a statistically significant increase. **(B)** Enriched nuclear proteins at days 2 and 16 showed the highest increase in their expression ratio, 60% and 54% of the proteins quantified had a statistically significant increase. **(C)** The cytosolic proteins were the least effected by glycemic stress, although about 34% of 16 days of showed a statistical significant increase. The horizontal line at the 1.3 ratio indicates a statistically significant change in protein level expression ($p < .05$).

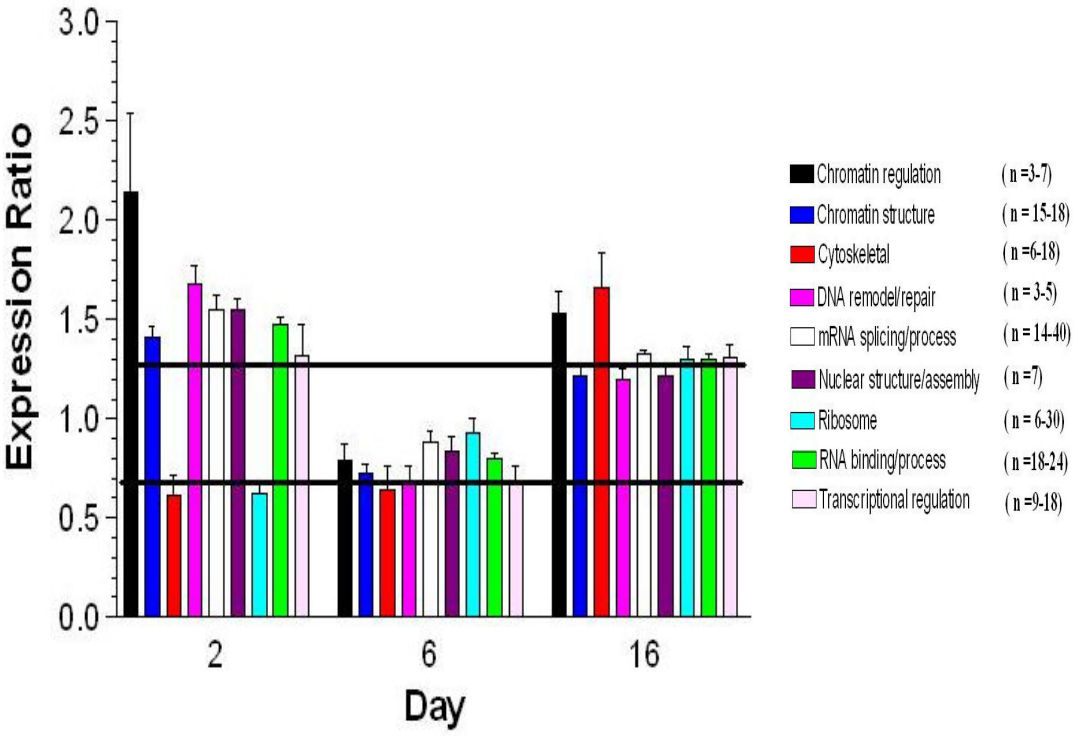

Figure 8. Proteins are Overexpressed That Play Crucial Roles in Protein Transcription. Clustering the quantified proteins into functional classes reveals that proteins involved in transcription are overexpressed. Similarly, mRNA splicing and RNA binding proteins were also overexpressed at 2 and 16 days, with an expression ratio greater than 1.3. The horizontal line at the 1.3 ratio indicates a statistically significant change in protein level expression ($p < .05$). (n represents the number of proteins that were quantified for each functional class).

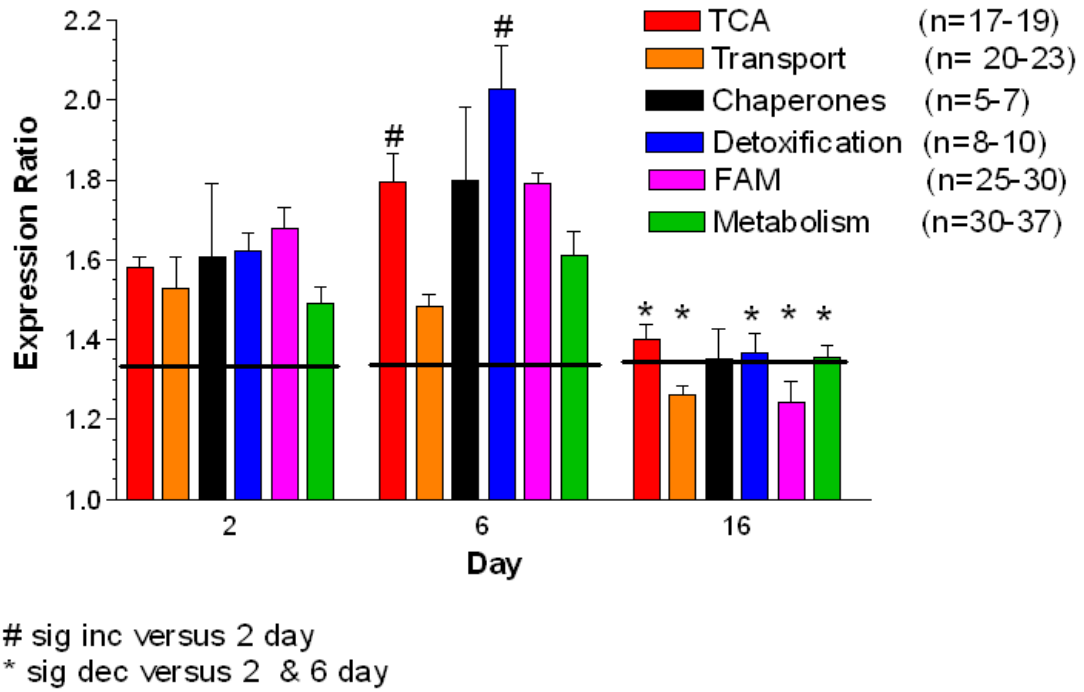

Figure 9. TCA and Detoxification Proteins are Overexpressed Under Chronic Hyperglycemia. Clustering the quantified proteins into functional classes reveals that proteins involved in glucose oxidation are overexpressed. Moreover, the byproduct of glucose metabolism leads to the generation of waste products and the cell responds by a robust expression of enzymes that detoxify, such as MnSOD. The asterisk denotes that at day 16, the proteins of each functional class decreased in expression relative to days 2 and 6. The horizontal line at the 1.3 ratio indicates a statistically significant change in protein level expression ($p < .05$). (n represents the number of proteins that were quantified for each functional class).

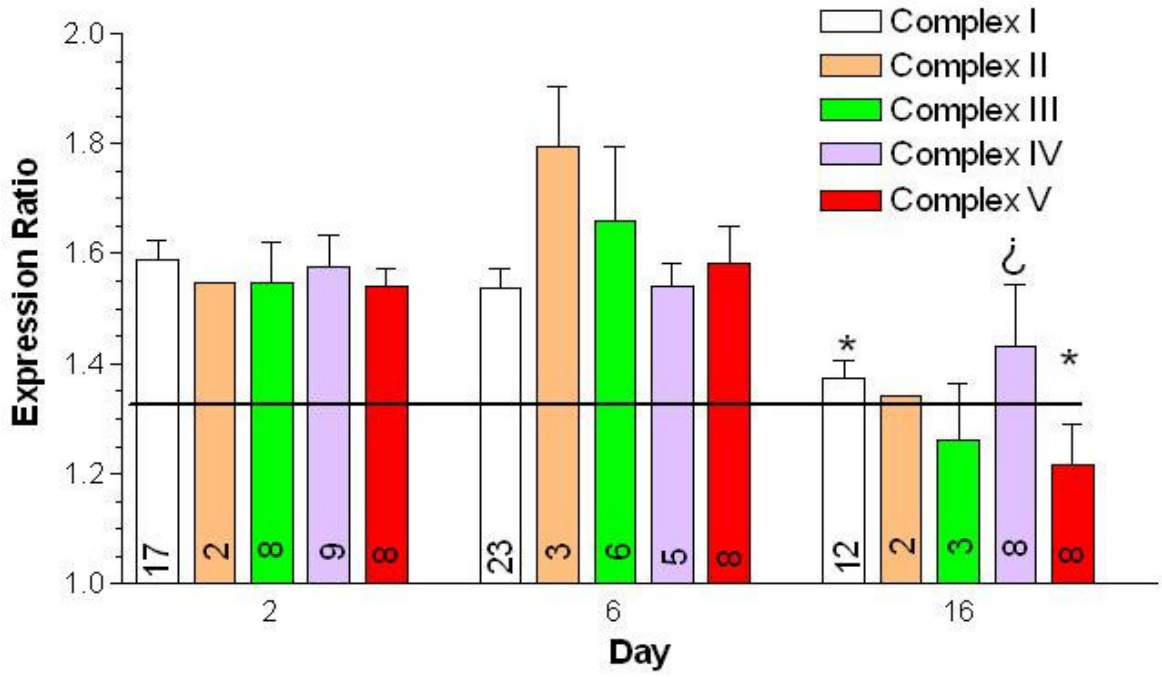

Figure 10. Chronic Hyperglycemia Induced Changes in Oxidative Phosphorylation Proteins. The primary site of glucose oxidation occurs in the TCA cycle generating excess FADH and $NADH_2$. Increase levels of reducing equivalents must be oxidized by complexes I through V, in which mass spectrometric analysis revealed increased expression ratio of the various subunits of each of the five complexes quantified. Notably, days 2 and 6 had the most proteins with a statistically significant expression ratio. The horizontal line at the 1.3 ratio indicates a statistically significant change in protein level expression ($p < .05$). The asterisk for complexes I and V at day 16 denotes a statistically significant decreased in expression relative to days 2 and 6 for the same complexes. The upside down question mark for complex IV at day 16 denotes a statistically significant decreased in expression ratio relative to day 2 for the same complex. (The number in the bars indicates the different subunits quantified for the particular complex)

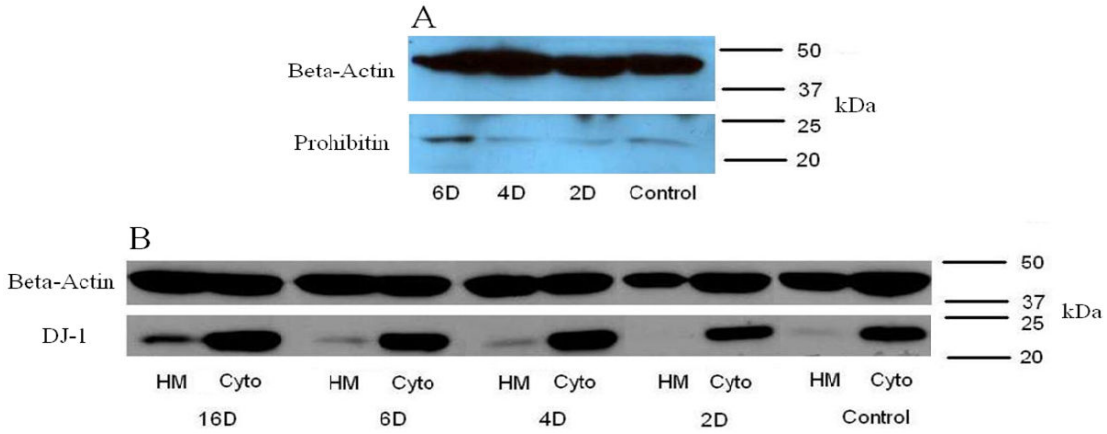

Figure 11. Overexpression of Prohibitin and DJ-1 Due to Glycemic Stress.
(A) Eight micrograms of total protein from the HM fraction of glucose stressed primary SCs were separated on SDS-PAGE and probed for prohibitin. Chronic hyperglycemia increased the expression of prohibitin, in line with the results obtained from mass spectrometry. β-actin was used as a loading control. **(B)** Eight micrograms of total protein from the HM and cytosolic fractions of glucose stressed primary SCs were separated on SDS-PAGE and probed for DJ-1. Chronic hyperglycemia induced the relocalization of cytosolic DJ-1 pools into the mitochondria. β-actin was used as a loading control. (HM = heavy mitochondria fraction, Cyto = cytosol fraction)

C

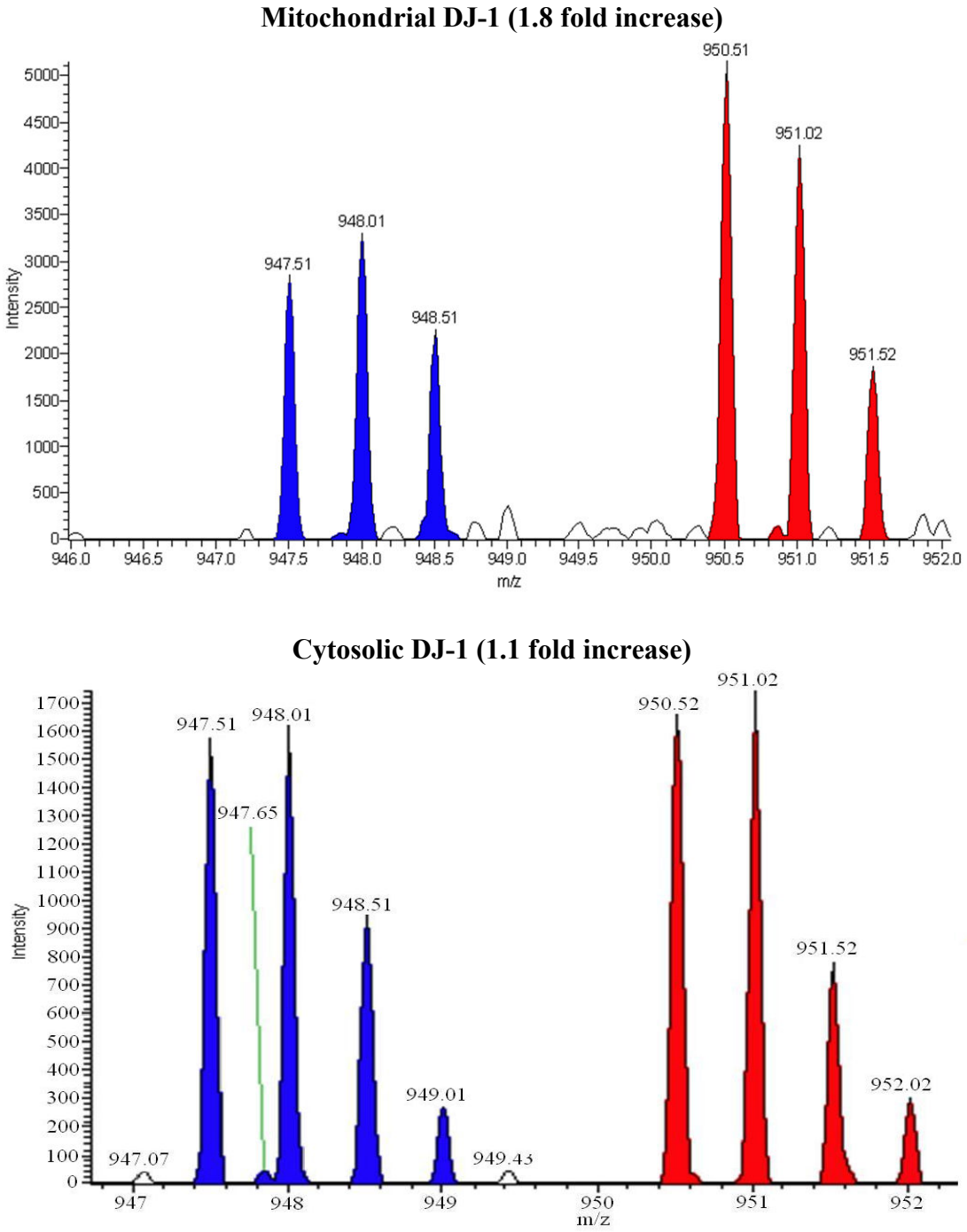

Figure 11 continued. Overexpression of Prohibitin and DJ-1 Due to Glycemic Stress. (C) Similar to the data obtained from the immunoblot, cytosolic pools of DJ-1 appear to be the least altered. In contrast, mitochondrial pools of DJ-1 consistently increase as hyperglycemic conditions are prolonged.

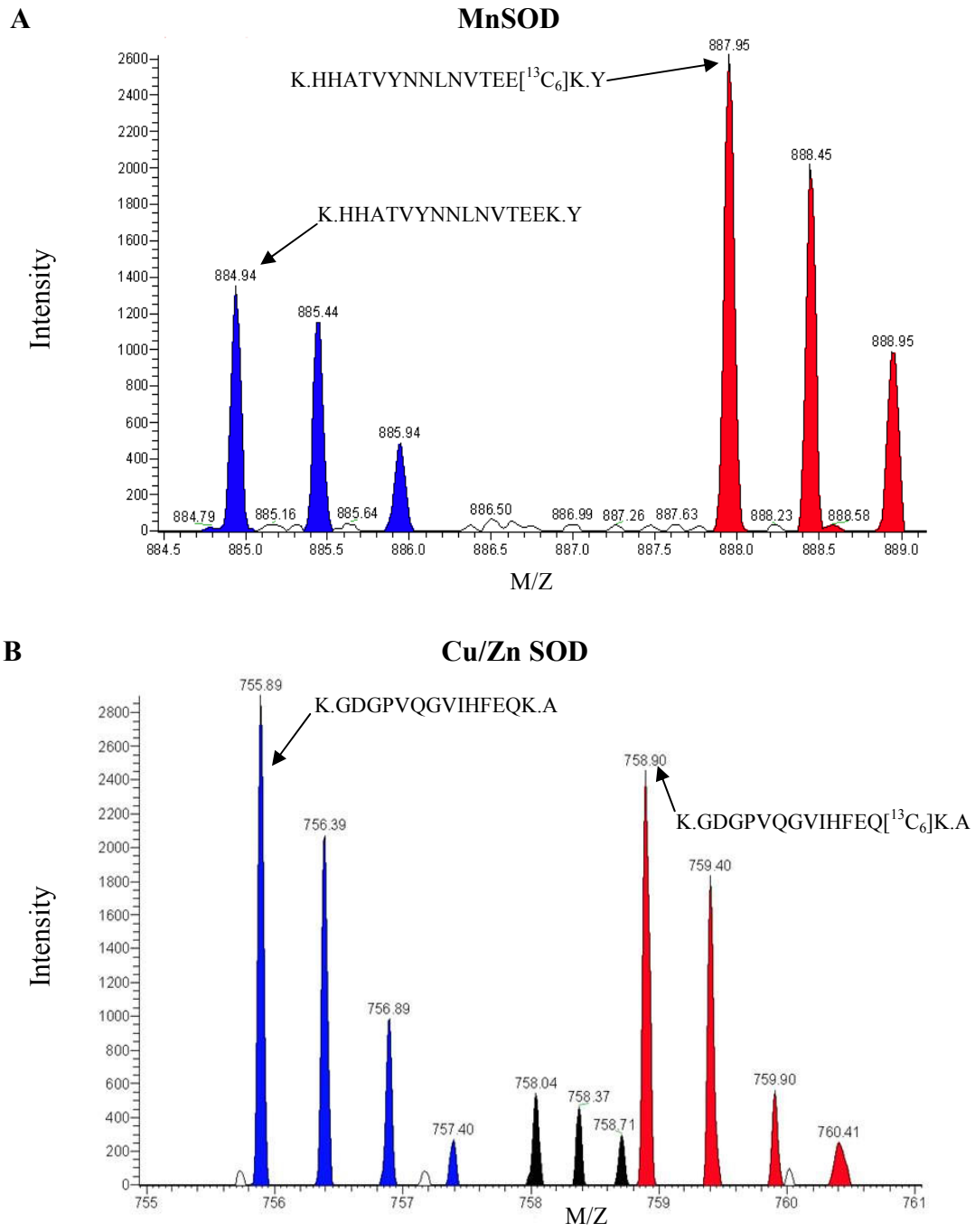

Figure 12. Variable Effects of Chronic Hyperglycemia on MnSOD and Cu/Zn SOD. (A). The mass spectra for the peptide sequence of MnSOD analyzed at day 6 of glycemic stress. At day 6, the expression ratio was 2.0 for the peptide sequence illustrated. **(B).** The cytosolic resident Cu/Zn SOD did not change significantly at day 6 of analysis. The peptide sequence of the dismutase pictured was 0.84. The triple charge peptide shown on the Cu/Zn SOD spectra is unrelated because of the incorrect m/z.

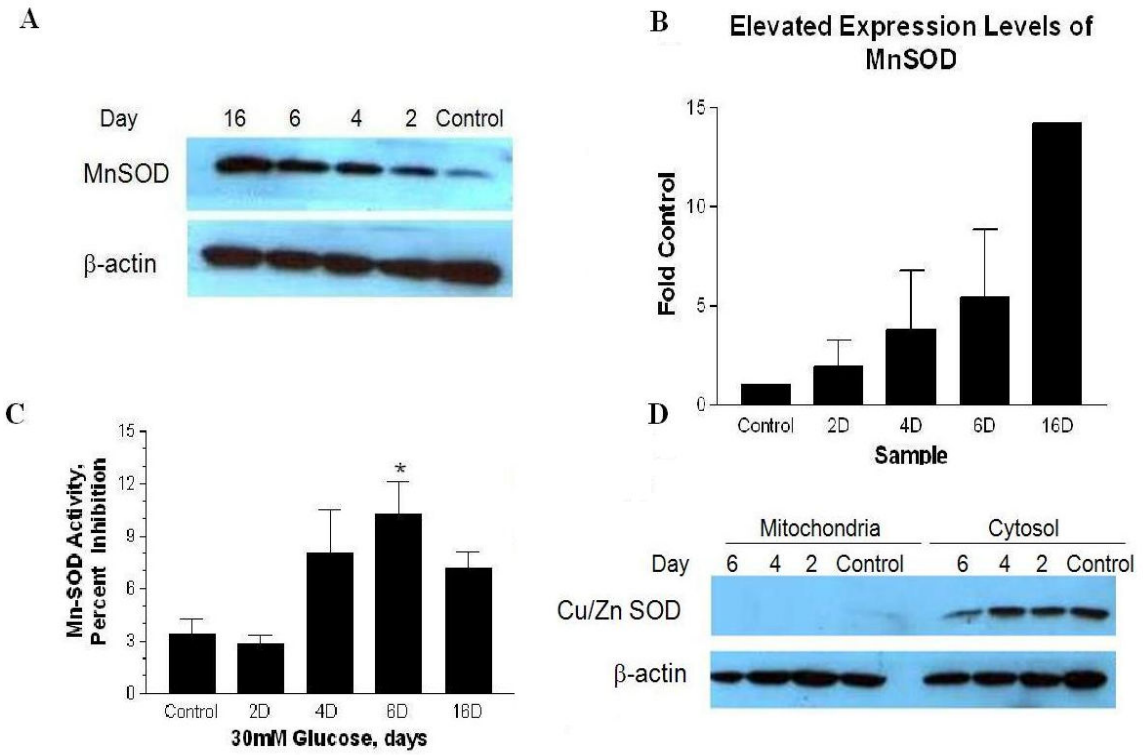

Figure 13. Chronic Hyperglycemia Correlates with Overexpression and Increased Activity of MnSOD. (A) Eight micrograms of total protein were separated on SDS-PAGE and immunoblotted for MnSOD and β-actin. By increasing the days of hyperglycemic stress, the SCs responds to high glucose by overexpressing MnSOD. **(B)** The graph depicts densitrometric analysis of the immunoblot data. The intensities of MnSOD were normalized against β-actin for each sample. The results shown are for 3 different experiments of chronic hyperglycemia up to 6 days. Only one experiment was extended out to 16 days. **(C)** A sample of the HM fraction was used to perform the SOD activity assay. Total protein used for the SOD assay ranged between .5 to 3 micrograms of protein. Each sample was assayed in triplicate for each of the three experiments. **(D)** Eight micrograms of the HM and cytosolic fractions were separated on SDS-PAGE and immunoblotted for Cu/Zn SOD. The HM fraction did not contain any detectable Cu/Zn SOD. As expected the cytosolic fraction did contain the Cu/Zn SOD, but no observable increase of the enzyme was noted. β-actin was used as a loading control.

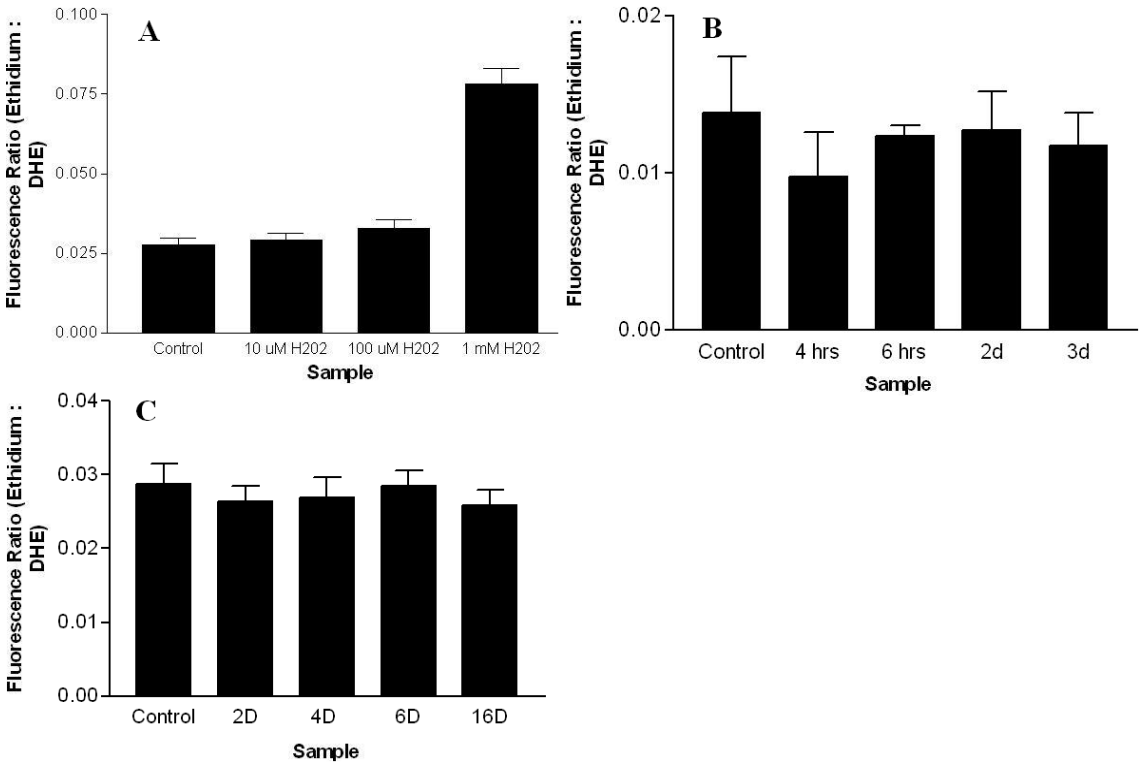

Figure 14. Acute and Chronic Hyperglycemia Failed to Induce Increased O_2^- Levels. **(A)** Hydrogen peroxide was used as a positive control to induce the generation of O_2^-. 15 minute incubation of primary SCs with 1 mM H202 generated a substantial increase of O_2^-**. (B)** Primary SCs were cultured in 30 mM glucose for the indicated acute and chronic conditions. Acute and chronic incubation periods of hyperglycemia failed to produce any statistically significant increase in O_2^-. **(C)** Primary SCs were cultured in 30 mM glucose for the indicated chronic conditions. Each chronic condition failed to produce a significant increase in O_2^- generation. The ratio of fluorescence is the emission value of ethidium over the emission value of DHE. The data presented is the average of three independent experiments with their relative standard error.

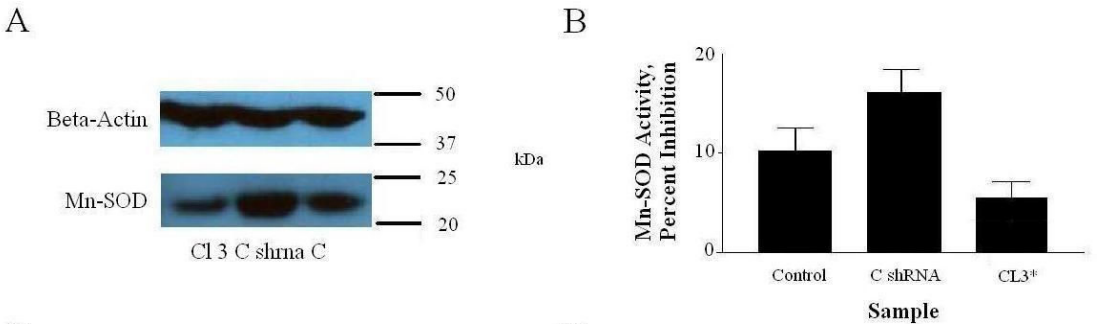

Figure 15. Decreased Protein Levels and Activity of MnSOD after shRNA Knockdown. (A) 8 ug of total protein from the HM fraction was separated by SDS-PAGE. After two days incubation with the lentivirus, the SCs were harvested and immunoblotted for MnSOD. Cl3 shows a significant reduction in MnSOD expression levels. **(B)** 1 – 3 ug of total protein of the same fraction used in Fig. 15a was assayed for SOD activity. Clearly there was a significant reduction in SOD activity on the Cl3 sample. C = non-infected cells. C shrna = lentivirus containing shRNA sequence with non- complementary sequence against MnSOD. Cl3 = lentivirus containing shRNA with a complementary sequence to mRNA of MnSOD. 65 µl of stock lentivirus was diluted in 5 mL of cell culture media.

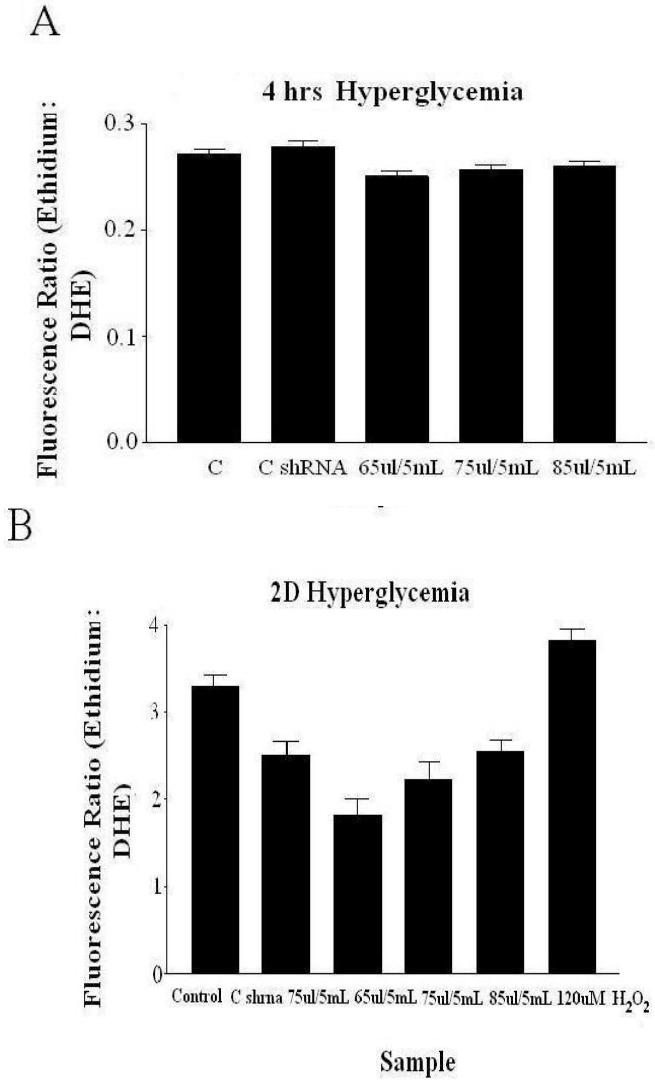

Figure 16. Absence of Increased O_2^- Levels after shRNA MnSOD Knockdown. **(A)** After 2 day of lentiviral infection, SCs were stressed acutely with 30 mM glucose. No significant O_2^- elevation was observed. **(B)** After 2 day of lentiviral infection, SCs were stressed chronically with 30 mM glucose. No significant O_2^- elevation was observed. **(C)** After 2 day of lentiviral infection, SCs were stressed chronically with 30 mM glucose. SCs destined for hydrogen peroxide (H_20_2) treatment were also subject to lentiviral infection. H_2O_2 caused a significant increase in O_2^- levels. Cl3 was an arbitrary assignation to the sequence described in the materials and methods section. C = non-infected cells. C shrna = lentivirus containing shRNA sequence with non- complementary sequence against MnSOD. Cl3 = lentivirus containing shRNA with a complementary sequence to mRNA of MnSOD. 65, 75, and 85 µl of stock lentivirus was diluted in 5 mL of cell culture media.

C

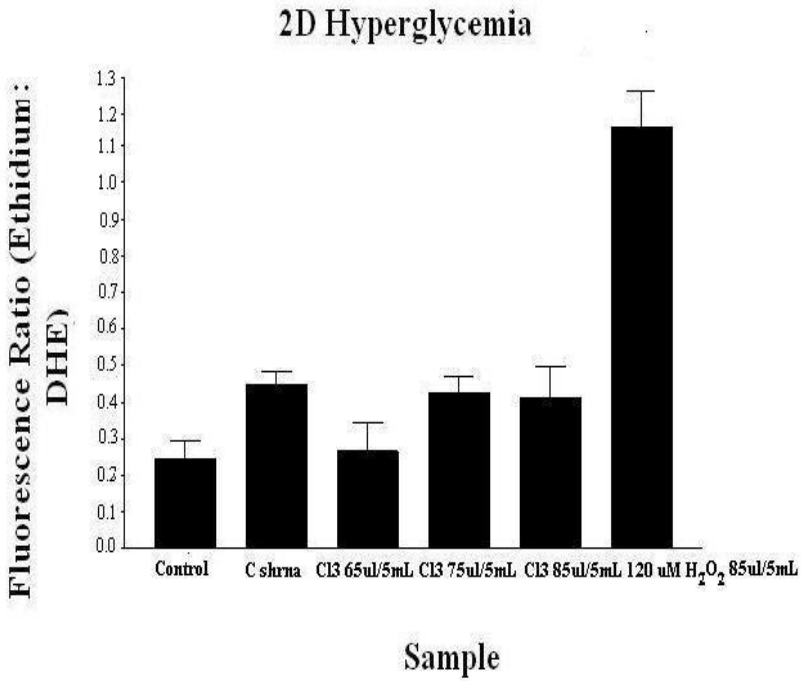

Figure 16 continued. Absence of Increased O_2^- Levels after shRNA MnSOD Knockdown. (C) After 2 day of lentiviral infection, SCs were stressed chronically with 30 mM glucose. SCs destined for hydrogen peroxide (H_20_2) treatment were also subject to lentiviral infection. H_2O_2 caused a significant increase in O_2^- levels. Cl3 was an arbitrary assignation to the sequence described in the materials and methods section. C = non-infected cells. C shrna = lentivirus containing shRNA sequence with non- complementary sequence against MnSOD. Cl3 = lentivirus containing shRNA with a complementary sequence to mRNA of MnSOD. 65, 75, and 85 µl of stock lentivirus was diluted in 5 mL of cell culture media.

References

1. *American Diabetes Association Diagnosis and classification of diabetes mellitus* Diabetes Care, 2007. **Suppl 1**: p. S42–S47.
2. Pradhan, A., *Obesity, metabolic syndrome, and type 2 diabetes: inflammatory basis of glucose metabolic disorders.* Nutr Rev, 2007. **65**(12 Pt 2): p. S152-6.
3. Lombard, L., *The management of type II diabetes.* SADJ, 2005. **60**(3): p. 120-1.
4. Reynolds, S.S., et al., *Glucose levels in the normal range predict incident diabetes in families with premature coronary heart disease.* Diabetes Res Clin Pract, 2006. **74**(3): p. 267-73.
5. Worrall, G., *Results of the DCCT trial. Implications for managing our patients with diabetes.* Can Fam Physician, 1994. **40**: p. 1955-60, 1963-5.
6. Martin, C.L., et al., *Neuropathy among the diabetes control and complications trial cohort 8 years after trial completion.* Diabetes Care, 2006. **29**(2): p. 340-4.
7. Marchettini, P., et al., *Painful peripheral neuropathies.* Curr Neuropharmacol, 2006. **4**(3): p. 175-81.
8. Watkins, P.J. and P.K. Thomas, *Diabetes mellitus and the nervous system.* J Neurol Neurosurg Psychiatry, 1998. **65**(5): p. 620-32.
9. Zolli, A., *Foot ulceration due to arterial insufficiency: role of cilostazol.* J Wound Care, 2004. **13**(2): p. 45-7.
10. Kidd, P.M., *Glutathione: systemic protectant against oxidative and free radical damage.* Journal of Clinical Therapeutics, 1997. **2**: p. 155-176.
11. Ho, E.C., et al., *Aldose reductase-deficient mice are protected from delayed motor nerve conduction velocity, increased c-Jun NH2-terminal kinase activation, depletion of reduced glutathione, increased superoxide accumulation, and DNA damage.* Diabetes, 2006. **55**(7): p. 1946-53.
12. Srivastava, S.K., K.V. Ramana, and A. Bhatnagar, *Role of aldose reductase and oxidative damage in diabetes and the consequent potential for therapeutic options.* Endocr Rev, 2005. **26**(3): p. 380-92.
13. Yamagishi, S., et al., *Agents that block advanced glycation end product (AGE)-RAGE (receptor for AGEs)-oxidative stress system: a novel therapeutic strategy for diabetic vascular complications.* Expert Opin Investig Drugs, 2008. **17**(7): p. 983-96.
14. Takenaka, K., et al., *Role of advanced glycation end products (AGEs) in thrombogenic abnormalities in diabetes.* Curr Neurovasc Res, 2006. **3**(1): p. 73-7.
15. Colaco, C.A. and B.J. Roser, *Atherosclerosis and glycation.* Bioessays, 1994. **16**(2): p. 145-7.

16. Schmidt, A.M. and D. Stern, *Atherosclerosis and diabetes: the RAGE connection.* Curr Atheroscler Rep, 2000. **2**(5): p. 430-6.
17. Bolton, W.K., et al., *Randomized trial of an inhibitor of formation of advanced glycation end products in diabetic nephropathy.* Am J Nephrol, 2004. **24**(1): p. 32-40.
18. Nakamura, S., et al., *Pyridoxal phosphate prevents progression of diabetic nephropathy.* Nephrol Dial Transplant, 2007. **22**(8): p. 2165-74.
19. Barile, G.R., et al., *The RAGE axis in early diabetic retinopathy.* Invest Ophthalmol Vis Sci, 2005. **46**(8): p. 2916-24.
20. Liang, Q., et al., *Elevated hexokinase increases cardiac glycolysis in transgenic mice.* Cardiovasc Res, 2002. **53**(2): p. 423-30.
21. Barnes, S.J. and P.D. Weitzman, *Organization of citric acid cycle enzymes into a multienzyme cluster.* FEBS Lett, 1986. **201**(2): p. 267-70.
22. Brownlee, M., *Biochemistry and molecular cell biology of diabetic complications.* Nature, 2001. **414**(6865): p. 813-20.
23. Wang, W., et al., *Superoxide flashes in single mitochondria.* Cell, 2008. **134**(2): p. 279-90.
24. Vinas, J.L., A. Sola, and G. Hotter, *Mitochondrial NOS upregulation during renal I/R causes apoptosis in a peroxynitrite-dependent manner.* Kidney Int, 2006. **69**(8): p. 1403-9.
25. Boyd, C.S. and E. Cadenas, *Nitric oxide and cell signaling pathways in mitochondrial-dependent apoptosis.* Biol Chem, 2002. **383**(3-4): p. 411-23.
26. Virag, L., et al., *Peroxynitrite-induced cytotoxicity: mechanism and opportunities for intervention.* Toxicol Lett, 2003. **140-141**: p. 113-24.
27. Kim, J.S., L. He, and J.J. Lemasters, *Mitochondrial permeability transition: a common pathway to necrosis and apoptosis.* Biochem Biophys Res Commun, 2003. **304**(3): p. 463-70.
28. Bax, J.J., et al., *Screening for coronary artery disease in patients with diabetes.* Diabetes Care, 2007. **30**(10): p. 2729-36.
29. Martini, R., *The effect of myelinating Schwann cells on axons.* Muscle Nerve, 2001. **24**(4): p. 456-66.
30. Vabnick, I. and P. Shrager, *Ion channel redistribution and function during development of the myelinated axon.* J Neurobiol, 1998. **37**(1): p. 80-96.
31. Bjartmar, C., X. Yin, and B.D. Trapp, *Axonal pathology in myelin disorders.* J Neurocytol, 1999. **28**(4-5): p. 383-95.
32. Blagoev, B., et al., *A proteomics strategy to elucidate functional protein-protein interactions applied to EGF signaling.* Nat Biotechnol, 2003. **21**(3): p. 315-8.
33. Ong, S.E., et al., *Stable isotope labeling by amino acids in cell culture, SILAC, as a simple and accurate approach to expression proteomics.* Mol Cell Proteomics, 2002. **1**(5): p. 376-86.
34. Schmidt, F., et al., *Rapid determination of amino acid incorporation by stable isotope labeling with amino acids in cell culture (SILAC).* Rapid Commun Mass Spectrom, 2007. **21**(23): p. 3919-26.

35. Ong, S.E., I. Kratchmarova, and M. Mann, *Properties of 13C-substituted arginine in stable isotope labeling by amino acids in cell culture (SILAC).* J Proteome Res, 2003. **2**(2): p. 173-81.
36. Bogdanov, B. and R.D. Smith, *Proteomics by FTICR mass spectrometry: top down and bottom up.* Mass Spectrom Rev, 2005. **24**(2): p. 168-200.
37. Hwang, S.I., et al., *Systematic characterization of nuclear proteome during apoptosis: a quantitative proteomic study by differential extraction and stable isotope labeling.* Mol Cell Proteomics, 2006. **5**(6): p. 1131-45.
38. Foster, L.J., et al., *Insulin-dependent interactions of proteins with GLUT4 revealed through stable isotope labeling by amino acids in cell culture (SILAC).* J Proteome Res, 2006. **5**(1): p. 64-75.
39. Nijtmans, L.G., et al., *Prohibitins act as a membrane-bound chaperone for the stabilization of mitochondrial proteins.* Embo J, 2000. **19**(11): p. 2444-51.
40. Geetha, T. and M.W. Wooten, *Structure and functional properties of the ubiquitin binding protein p62.* FEBS Lett, 2002. **512**(1-3): p. 19-24.
41. Johnson, M.K. and V.P. Whittaker, *Lactate Dehydrogenase as a Cytoplasmic Marker in Brain.* Biochem J, 1963. **88**: p. 404-9.
42. Quinones, Q.J., G.G. de Ridder, and S.V. Pizzo, *GRP78: a chaperone with diverse roles beyond the endoplasmic reticulum.* Histol Histopathol, 2008. **23**(11): p. 1409-16.
43. Konat, G.W., *H2O2-induced higher order chromatin degradation: a novel mechanism of oxidative genotoxicity.* J Biosci, 2003. **28**(1): p. 57-60.
44. Mouzannar, R., et al., *Hydrogen peroxide induces rapid digestion of oligodendrocyte chromatin into high molecular weight fragments.* Neurochem Int, 2001. **38**(1): p. 9-15.
45. Lorenzi, M., E. Cagliero, and S. Toledo, *Glucose toxicity for human endothelial cells in culture. Delayed replication, disturbed cell cycle, and accelerated death.* Diabetes, 1985. **34**(7): p. 621-7.
46. Schleicher, M., et al., *Prohibitin-1 maintains the angiogenic capacity of endothelial cells by regulating mitochondrial function and senescence.* J Cell Biol, 2008. **180**(1): p. 101-12.
47. Taira, T., et al., *DJ-1 has a role in antioxidative stress to prevent cell death.* EMBO Rep, 2004. **5**(2): p. 213-8.
48. Canet-Aviles, R.M., et al., *The Parkinson's disease protein DJ-1 is neuroprotective due to cysteine-sulfinic acid-driven mitochondrial localization.* Proc Natl Acad Sci U S A, 2004. **101**(24): p. 9103-8.
49. Flanagan, S.W., et al., *Overexpression of manganese superoxide dismutase attenuates neuronal death in human cells expressing mutant (G37R) Cu/Zn-superoxide dismutase.* J Neurochem, 2002. **81**(1): p. 170-7.
50. Vincent, A.M., M. Brownlee, and J.W. Russell, *Oxidative stress and programmed cell death in diabetic neuropathy.* Ann N Y Acad Sci, 2002. **959**: p. 368-83.

51. Cosentino, F., et al., *High glucose increases nitric oxide synthase expression and superoxide anion generation in human aortic endothelial cells.* Circulation, 1997. **96**(1): p. 25-8.
52. Robertson, R.P., et al., *Glucose toxicity in beta-cells: type 2 diabetes, good radicals gone bad, and the glutathione connection.* Diabetes, 2003. **52**(3): p. 581-7.
53. Greene, D.A. and A.I. Winegrad, *In vitro studies of the substrates for energy production and the effects of insulin on glucose utilization in the neural components of peripheral nerve.* Diabetes, 1979. **28**(10): p. 878-87.
54. Magnani, P., et al., *Regulation of glucose transport in cultured Schwann cells.* J Peripher Nerv Syst, 1998. **3**(1): p. 28-36.
55. Zou, M.H., C. Shi, and R.A. Cohen, *High glucose via peroxynitrite causes tyrosine nitration and inactivation of prostacyclin synthase that is associated with thromboxane/prostaglandin H(2) receptor-mediated apoptosis and adhesion molecule expression in cultured human aortic endothelial cells.* Diabetes, 2002. **51**(1): p. 198-203.
56. Quijano, C., et al., *Enhanced mitochondrial superoxide in hyperglycemic endothelial cells: direct measurements and formation of hydrogen peroxide and peroxynitrite.* Am J Physiol Heart Circ Physiol, 2007. **293**(6): p. H3404-14.
57. Wu, F. and J.X. Wilson, *Peroxynitrite-dependent activation of protein phosphatase type 2A mediates microvascular endothelial barrier dysfunction.* Cardiovasc Res, 2008.
58. Kruger, M., et al., *SILAC mouse for quantitative proteomics uncovers kindlin-3 as an essential factor for red blood cell function.* Cell, 2008. **134**(2): p. 353-64.
59. Jandeleit-Dahm, K., A. Watson, and A. Soro-Paavonen, *The AGE/RAGE axis in diabetes-accelerated atherosclerosis.* Clin Exp Pharmacol Physiol, 2008. **35**(3): p. 329-34.